To the Graduate Council:

I am submitting herewith a thesis written by Jennifer L. Aponte entitled "Point Mutations in the Murine *Fah* Gene: Animal Models for the Human Genetic Disorder Hereditary Tyrosinemia Type 1." I have examined the final copy of this thesis for form and content and recommend that it be accepted in partial fulfillment of the requirements for the degree of Master of Science, with a major in Biomedical Sciences.

Dabney K. Johnson, Major Professor

We have read this thesis
and recommend its acceptance:

Accepted for the Council:

Associate Vice Chancellor and
Dean of the Graduate School

Point Mutations in the Murine *Fah* Gene: Animal Models for the Human Genetic Disorder Hereditary Tyrosinemia Type 1

A Thesis
Presented for the
Master of Science
Degree
The University of Tennessee,
Knoxville

Jennifer Lynn Aponte
May, 1997

DEDICATION

This thesis is dedicated to my husband

Carlos A. Aponte

who has given me invaluable love and support

and to the loving memory of my mother

Jennie Mae Harris.

ACKNOWLEDGEMENTS

I am grateful to many people at the University of Tennessee and Oak Ridge National Laboratory for their assistance during my graduate school experience. I would like to thank Dr. Dabney K. Johnson, my major advisor, for her advice and encouragement. I am also thankful for her technical assistance and guidance during the preparation of this thesis. I would like to thank the members of my committee, Drs. Margaret Terzaghi-Howe and Monica Justice for their time, guidance, and help in the preparation of this thesis.

I would also like to recognize additional people who have provided technical and personal support throughout the years. Dr. Gary Sega for his assistance with the succinylacetone analysis, Don Carpenter for his assistance in maintaining the mouse stocks, and Catherine Withrow for her experimental contributions. I would also like to express my appreciation to all the members of the laboratory. Troya Yoder, Kay Houser, Min Wu, Mitchell Walkowicz, Madhu Dhar have been an irreplaceable source of advice and encouragement in the laboratory and great friends. Finally, I would like to thank my entire family, including my husband, Carlos Aponte for their support and encouragement.

ABSTRACT

Hereditary tyrosinemia type 1 (HT1) is a severe autosomal recessive metabolic disease, associated with point mutations in the human fumarylacetoacetate hydrolase (*FAH*) gene that cause disruption of tyrosine catabolism. The acute form results in death during the first months of life due to hepatic failure, while the chronic form leads to gradual liver disease development often accompanied by renal dysfunction, childhood rickets, neurological crisis, and hepatocellular carcinoma. In the mouse, *Fah* maps near the *albino* (*c*) locus in chromosome 7. Mice homozygous for specific deletions around *c* that include *Fah* die perinatally as a result of liver dysfunction and exhibit a complex syndrome characterized by structural abnormalities of the liver and kidney, and alterations in gene expression. Here we report that two mutations induced by *N*-ethyl-*N*-nitrosourea (ENU) and mapped near *c* are alleles of *Fah*. The fah^{6287SB} allele is a missense mutation in exon 6 causing a reduction of *Fah* mRNA levels, and fah^{5961SB} is a splice mutation causing loss of exon 7, a subsequent frameshift in the resulting mRNA, and a severe reduction of *Fah* mRNA levels. The identification of mutations was determined by DNA sequencing, and *Fah* expression analysis was carried out by northern blot analysis. Increased levels of the diagnostic metabolite succinylacetone in the urine of the fah^{6287SB} and fah^{5961SB} mutants, identified by gas chromatography / mass spectrometry, indicates that the mutations cause a decrease in Fah enzymatic activity. Thus, the neonatal phenotype present in both mutants is due to a deficiency in Fah caused by a point mutation, and we propose fah^{5961SB} and fah^{6287SB} as mouse models for the acute and chronic forms of HT1, respectively.

TABLE OF CONTENTS

Part 1: Introduction

Background 2

The *Fah* Gene and *Albino* Deletion Mice 8

Research Objectives and General Overview 17

References 21

Part 2: Point Mutations in the Murine *Fah* Gene: Animal Models for the Human Genetic Disorder Hereditary Tyrosinemia Type 1

Abstract 27

Introduction 28

Results 34

Isolation of the *Fah* cDNAs and Identification of Point Mutations 34

Expression of the Normal *Fah* mRNA in the livers of fah^{5961SB} and fah^{6287SB} Mice 39

Neonathal Death of fah^{5961SB} and fah^{6287SB} Homozygotes and Hemizygotes 39

Biochemical Abnormality in fah^{5961SB} and fah^{6287SB} Mutant Mice 42

Discussion 45

Materials and Methods 49

Mice 49

RNA Isolation and Northern Blot Analysis 49

cDNA Production, PCR and Sequencing 50

PCR Amplification of Genomic DNA and Sequencing 50

Biochemical Analysis 51

References.....53

Appendix

Appendix A. Supplemental Data 57

Vita.....62

LIST OF FIGURES

Figure Page

Part 1: Introduction

1-1. Tyrosine degradation pathway 4

1-2. Schematic representation of the location of *hsdr1* on mouse chromosome 7 10

1-3. Breeding protocol for the detection of ENU-induced mutations in the *albino* region of mouse chromosome 7 15

1-4. Complementation mapping of the ENU-induced neonatal lethal mutations, fah^{5961SB} and fah^{6287SB}, within the *albino* region of mouse chromosome 7 18

Part 2: Point Mutations in the Murine *Fah* Gene: Animal Models for the Human Genetic Disorder Hereditary Tyrosinemia Type I

2-1. Complementation mapping of two ENU-induced neonatal lethal mutations within the *c* region of mouse chromosome 7 30

2-2. Nucleotide sequences of exons 6, 7, and 8 of control BALB/cRl, mutant fah^{6287SB}, and mutant fah^{5961SB} 35

2-3. Schematic representation of the fah^{5961SB} mutation, and its effect on the processing of the *Fah* mRNA 37

2-4. Northern blot analysis of the *Fah* gene 40

2-5. Bar graph showing SA levels in urine of fah^{5961SB}, fah^{6287SB} and control mice 43

Appendix

A-1. Analysis of fah^{5961SB} and BALB/cRl cDNAs 58

A-2. Northern blot analysis of liver RNA from fah^{6287SB} mice 60

LIST OF ABBREVIATIONS

c	*albino*
cAMP	cyclic AMP
c^{ch}	*chinchilla*
cDNA	complementary DNA
DNA	deoxyribonucleic acid
E	glutamic acid
ENU	*N*-ethyl-*N*-nitrosourea
FAA	fumarylacetoacetate
FAH	fumarylacetoacetate hydrolase (human enzyme)
FAH	*fumarylacetoacetate hydrolase* (human gene)
Fah	fumarylacetoacetate hydrolase (murine enzyme)
Fah	*fumarylacetoacetate hydrolase* (murine gene)
G	glycine
gadd	growth arrest DNA damage
GC/MS	gas chromatography / mass spectrometry
HGA	homogentisic acid
HPLC	high pressure liquid chromatography
hsdr1	*hepatocyte-specific developmental regulation-1*
HT1	hereditary tyrosinemia type 1
IRM	immunoreactive material
IVS	intervening sequence

MAA	maleylacetoacetate
mRNA	messenger RNA
NaCl	sodium chloride
NMO-1	menadione oxidoreductase
NTBC	2-(2-nitro-4-trifluoro-methylbenzyol)-1,3-cyclohexanedione
ORF	open reading frame
PCR	polymerase chain reaction
RNA	ribonucleic acid
RT	reverse transcriptase
SA	succinylacetone
SDS	sodium dodecyl sulfate
SIM	selective ion monitoring
SLT	specific locus test
SSCP	sodium citrate sodium phosphate

Part 1

Introduction

BACKGROUND

Hereditary tyrosinemia type 1 (HT1) is an autosomal recessive disease caused by a deficiency of fumarylacetoacetate hydrolase (FAH), the last enzyme in the catabolic pathway of tyrosine[1]. There are two general forms of the disease; acute HT, where patients have an absence of detectable FAH, and chronic HT, where individuals have reduced FAH levels (~20%-30% of normal). Some of the many clinical characteristics include structural abnormalities of the liver and kidney, hypertyrosinemia, progressive liver damage (chronic patients), liver dysfunction, hepatic tumors and cirrhosis, renal dysfunction, and neurological crisis (~40% of patients)[2,3]. Patients also show increased concentrations of tyrosine in the blood, increased concentrations of tyrosine and tyrosine metabolites (succinylacetone, succinylacetoacetate) in urine, increased concentrations of δ-aminolevulinic acid in urine, and hypermethioninemia[2].

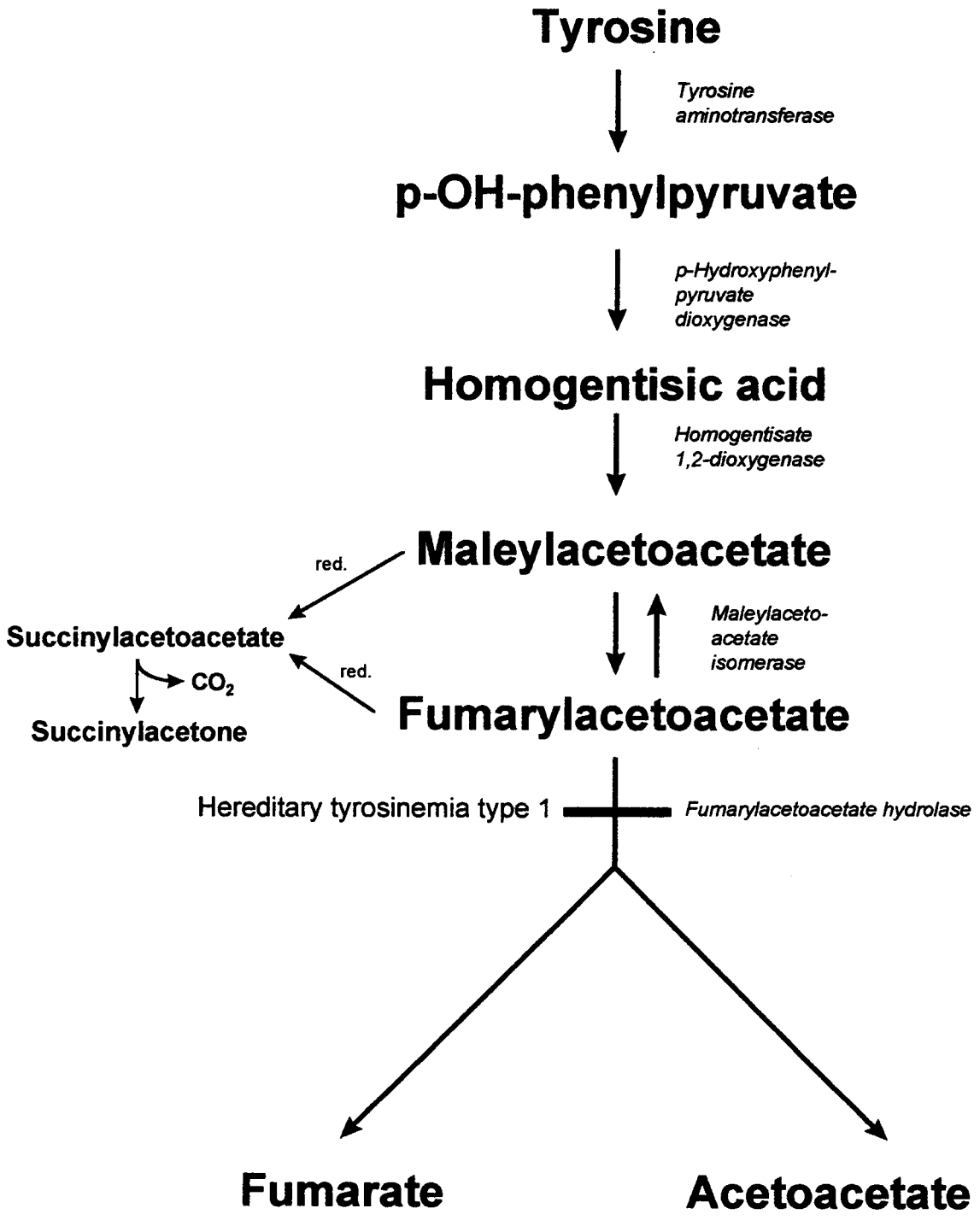
The acute, early onset form of the disease is the type most frequently reported. Symptoms appear during the first months of life with a general failure to thrive; these individuals lacking FAH have severe symptoms and usually die from liver failure in the first months of life if not treated. The chronic form, with later onset and milder features, results in gradual liver disease development in which individuals suffer from renal tubule dysfunctions, vitamin D-resistant rickets and often develop hepatocarcinoma in their teens. Patients with the chronic disease have detectable levels of FAH[4]. The disorder occurs worldwide but the frequency is variable, with a high incidence in the French Canadian and Scandinavian populations[5].

The primary deficiency of FAH leads to the clinical manifestations in patients via

secondary responses. Fumarylacetoacetate (FAA), maleylacetoacetate (MAA) and succinylacetone (SA) accumulate as a result of the primary deficiency of FAH[6] (Figure 1-1), and these metabolites are believed to be responsible for certain pathological aspects of the disorder[6,7]. The clinical manifestations arise primarily in the liver and kidney because these are the areas of highest *FAH* expression and, thus, the areas of local metabolite buildup. SA metabolite accumulation causes inhibition of renal tubule transport of amino acids and glucose, which may cause the tubulopathy seen in the disorder[1]. MAA and FAA are natural alkylating agents[2] and are believed to cause chromosomal breakage and cellular damage. This genetic instability may be related to the development of tumors and to the dysplastic changes seen in HT1 patients[3]. SA and FAA also cause inhibition of some vital secondary enzymes, including δ-aminolevulinic dehydratase and methionine adenosyltransferase[6]. The first enzyme, δ-aminolevulinic dehydratase, is an enzyme of heme synthesis, and abnormal heme synthesis causes neurological crisis and has also been linked to the initiation of carcinogenesis[8]. Aminolevulinic dehydratase inhibition is responsible for the increased excretion of aminolevulinic acid seen in HT1 patients[8]. Inhibition of methionine adenosyltransferase results in hyper-methioninemia (acute state) and may also cause hypomethylation of DNA, which can lead to carcinogenesis[2].

In addition to inhibiting renal and enzyme functions, SA has also been found to react nonenzymatically with amino acids, proteins, and glutathione to form stable adducts. Adduct formation with glutathione leads to decreased glutathione levels, which can interfer with glutathione-dependent detoxification mechanisms and contribute to less

Figure 1-1. Tyrosine degradation pathway. A deficiency of *FAH* is the primary enzyme defect in hereditary tyrosinemia type 1. This deficiency results in the accumulation of fumarylacetoacetate and maleylacetoacetate, which are reduced and decarboxylated to yield succinylacetone.


Tyrosine
Tyrosine aminotransferase
p-OH-phenylpyruvate
p-Hydroxyphenyl-pyruvate dioxygenase
Homogentisic acid
Homogentisate 1,2-dioxygenase
Maleylacetoacetate
red.
Maleylaceto-acetate isomerase
Succinylacetoacetate
red.
CO_2
Succinylacetone
Fumarylacetoacetate
Hereditary tyrosinemia type 1
Fumarylacetoacetate hydrolase
Fumarate
Acetoacetate

efficient protection against cell injury[1]. SA adduct formation occurs in tyrosinemia and may account for certain of the pathological findings in the disorder[9]. It appears that the carcinogenesis aspect of HT1 may be a combined response, the result of the reduction in cell protective agents (glutathione, for example), the hypomethylation of DNA, and the inhibition of various enzymes.

SA is considered to be the hallmark metabolite for HT1 because elevation of SA above normal levels (in serum, urine, and/or amniotic fluid) is indicative and specific for the disease. Increase in SA levels is unique to this disorder[2,10] so that measurement of SA can be used as a diagnostic tool for HT1[6,11,12]. Diagnosis of HT1 can also be made by assaying FAH activity in amniocytes, chorionic villus material[13], lymphocytes, and fibroblasts; these cell types express *FAH*, although only the liver and kidney contain the complete set of enzymes required for tyrosine degradation. In addition, a number of restriction fragment length polymorphisms in the *FAH* gene have been described and used for carrier and prenatal diagnosis[14].

Once the diagnosis of HT1 has been established, various treatment methods can be utilized. Dietary restriction of tyrosine and phenylalanine has been found to alleviate the rickets but does not cure the liver disease[2]. Liver transplantation has been the most effective treatment thus far. A recently reported treatment uses the drug 2-(2-nitro-4-trifluoro-methylbenzyol)-1,3-cyclohexanedione (NTBC) to inhibit 4-hydroxyphenylpyruvate dioxygenase, an enzyme that acts upstream of FAH in the catabolic pathway of tyrosine[12]. This inhibition reduces the accumulation of the hepatotoxins (FAA, MAA, SA) upstream of FAH. Laboratory signs indicate that after

NTBC treatment, patients appear to have improved liver function and a reduction in tubule damage. Gene therapy options are also presently under investigation[7].

The deficiency of FAH is found in both acute and chronic patients. Human patients with large deletions or rearrangements in *FAH* have not been found, suggesting that small mutations are responsible for the disease phenotype. At least 26 mutations have been reported in HT1 patients to date, including nonsense mutations, splice consensus site mutations, and missense mutations[5,15-20]. All are believed to decrease enzyme activity either by destabilizing the mutant enzyme or by altering its structure[17]. Different clinical forms result from the presence of these different molecular defects. Various molecular phenotypes exist [amount/presence of mRNA, amount of immunoreactive material (IRM), and amount of enzyme activity], and there is no apparent relationship between molecular and clinical phenotypes, except that individuals with no detectable FAH activity have an early onset[5,21]. The same molecular phenotype can be caused by different mutations and individuals with the same mutation (siblings) can have different clinical severities[5,13]. The ultimate severity of the disease seems to be correlated with the enzyme activity remaining in the liver[22]. The possible reasons for the clinical heterogeneity could be the genetic background of the patient, environmental factors, intercurrent infections, and different degrees of liver involvement (intoxification)[21,22].

The effect of specific mutations on the structure and/or function of FAH can only be hypothesized, since the structure of the FAH protein is unknown. What is known about the human FAH protein is that it is a homodimer consisting of two identical

monomers of molecular weight 43kD[22]. The gene maps to the long arm of chromosome 15 in the region q23-q25[23], covers 30 kilobases of DNA (13 introns and 14 exons), and has an open reading frame of ~1.3 kilobases in size[24].

THE *Fah* GENE AND *ALBINO* DELETION MICE

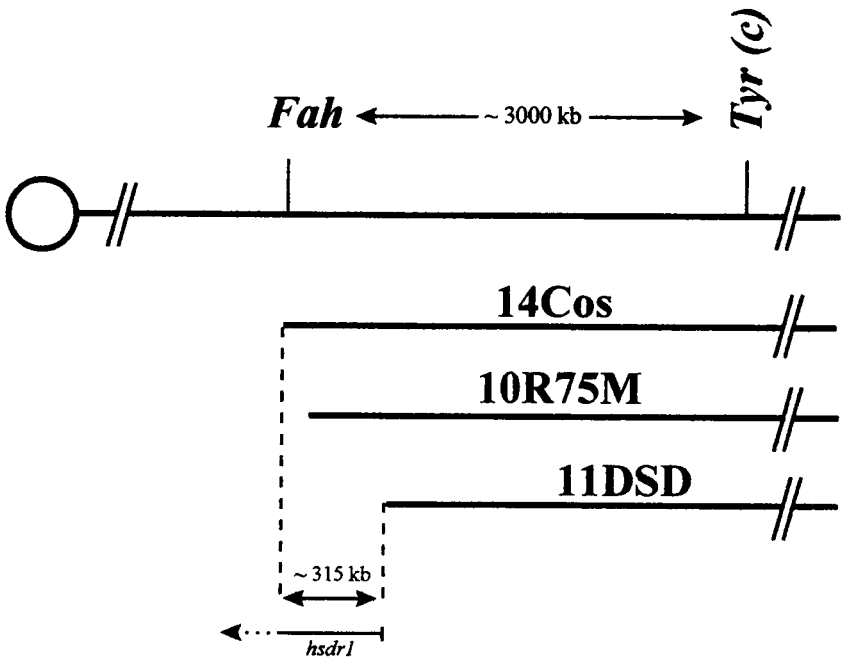
The *albino* (*c*) locus on mouse chromosome 7 was one of seven recessive marker loci used in mutation-rate experiments at Oak Ridge National Laboratory for the detection and quantification of heritable mutations in mammals. A complex of 37 overlapping radiation-induced deletions that remove the *c* locus and surrounding regions of chromosome 7 was derived from specific-locus mutagenesis experiments[25-27]. The general protocol followed in the specific locus test (SLT) was to expose a wild-type animal to a mutagen (ionizing radiation or chemicals) and mate the irradiated mouse to a strain homozygous for seven recessive genes; six specify coat color or pattern and the seventh reduces ear length. Mutant offspring can be easily detected simply by observation of coat color or ear size[27,28]; this test can also reveal dominant mutations at any loci.

Embryological and complementation analysis classified mutations at *c* into 13 groups that defined at least 6 loci necessary for either pre- or postnatal development[25,26,29,30]. Deletions belonging to one of the *albino* complementation groups identified a locus, *hsdr1* (*hepatocyte-specific developmental regulation-1*)[30] required for postnatal survival, since mice homozygous for certain deletions (ie. c^{14CoS}, c^{10R75M}) die during the first postnatal day as a result of hypoglycemia due to a failure to express high

neonatal levels of glucose-6 phosphatase and other enzymes in the liver and kidney associated with gluconeogenesis[30]. In wild-type animals, expression of these genes is induced around the time of birth by glucocorticoids and/or cAMP; however, this induction does not occur in the mutant mice[31-34]. The mice also exhibit a syndrome characterized by structural abnormalities of the liver and kidney, reduced levels of many liver- and kidney-specific enzymes and proteins, and increased transcription of enzymes involved in defending against oxidative stress and DNA damage[30,34-38]. These phenotypes are limited to hepatocytes and the proximal convoluted tubule cells of the kidney[34]. The structural genes for the affected enzymes do not map to the deletion complex[39] and glucocorticoid receptors and hormone levels are unaffected in the mutants[33]. These observations led to the hypothesis that the locus *hsdr1* is contained within the deletions and responsible for the syndrome[30]. It was proposed that *hsdr1* harbors regulatory gene(s) required for the perinatal activation of a set of hormone-inducible structural genes in the liver and kidney[30,32]. Since the phenotype is defined by a deletion interval, it was not known whether loss of one or more than one gene was responsible for the disease phenotype.

Complementation analysis using different overlapping deletions (ie., c^{11DSD}, c^{14CoS}, c^{112K}, c^{4PB}) showed that the c^{11DSD} deletion complements the c^{14CoS} disease phenotype[25], localizing *hsdr1* to the interval between the proximal breakpoint of c^{11DSD} and the proximal breakpoint of c^{14CoS}. The minimal region for *hsdr1* was then further defined to a 315-kb fragment at the proximal end of the c^{14CoS} deletion when those deletion breakpoints were identified molecularly[40-43] (Fig. 1-2). The first two exons of

Figure 1-2. Schematic representation of the location of *hsdr1* on mouse chromosome 7. Deletion breakpoint mapping identifies the ~315 kb interval within which the gene(s) responsible for the *hsdr1* deletion phenotype must be located. The candidate gene(s) may extend past the proximal breakpoint of the c^{14CoS} deletion, as is the case for the candidate gene *Fah* (see text). The c^{10R75M} deletion maps <1 kb 5' to the start of *Fah* transcription (see text). *Fah* is ~3000 kb from c^{41}. The circle on the *left* of the chromosome represents the centromere.


Fah
~ 3000 kb
Tyr (c)
14Cos
10R75M
11DSD
~ 315 kb
hsdr1

the gene encoding fumarylacetoacetate hydrolase (*Fah*) are deleted by the c^{14CoS} deletion, leading to the proposal of *Fah* as a candidate for *hsdr1*[34,43] (Fig. 1-2). A second deletion of interest is the c^{10R75M} deletion, which in the homozygous condition also disrupts the expression of the *Fah* gene. However, this deletion does not disrupt coding regions and its proximal breakpoint maps <1 kilobase 5' to the start site of transcription[34]. It was believed that the c^{10R75M} deletion may remove sequences essential for expression of *Fah*, and it has been reported that the deletion removes a DNaseI hypersensitive site in the liver and kidney chromatin causing the disruption of *Fah* expression in the mutants[34]. The murine *Fah* gene[34,43] has an open reading frame (ORF) of ~1.3 kilobases and has 13 exons and 12 introns[15,24]. Human *FAH* has 14 exons and 13 introns, whereas the mouse *Fah* has combined human exons 3 and 4 and lost intron 3 to form one exon instead of two, with all other exons identical in size. The murine ORF is 84% identical in sequence to the human ORF and has 94% similarity of amino acids predicted by the ORF[43].

Much circumstantial evidence has been presented indicating that loss of the *Fah* gene in the deletion mutants can account for all aspects of the *hsdr1* phenotype[34,37,44]. First, northern blot and *in situ* hybridization analysis of mouse tissues showed that the cell types that normally express *Fah* (parenchymal cells of the liver and proximal convoluted tubule cells of the kidney) correspond to those that exhibit the phenotype in *hsdr1* deletion mice[34]. Second, the *hsdr1* phenotype develops in c^{14CoS} homozygotes at day 16.5 of gestation, and *Fah* mRNA is expressed as early as fetal day 16 in both liver and kidney in wild-type mice[34]. Third, *hsdr1* deletion mice have reduced levels of many liver- and kidney-specific enzymes and proteins, including several enzymes involved in

gluconeogenesis (glucose-6 phosphatase, phosphoenolpyruvate carboxykinase, tyrosine aminotransferase), which may result from the toxic effects of the accumulating metabolites FAA and/or MAA. Cultured hepatocytes challenged with homogentisic acid (HGA, an intermediate of tyrosine metabolism) exhibit changes in gene expression similar to those in the liver of an animal carrying lethal *albino* deletions[34]. Fourth, *hsdr1* deletion mice have increased transcription of enzymes involved in defending against oxidative stress (menadione oxidoreductase, NMO-1), and enzymes associated with growth arrest and DNA damage (*gadd* transcripts). These responses may be induced in an attempt to detoxify the liver and kidney and repair damage. An increase in NMO-1 mRNA is induced in hepatocytes in response to HGA treatment, and c^{14CoS} hepatocytes display a much greater increase of NMO-1 mRNA compared to wild-type hepatocytes due to their inability to clear toxic metabolites.

Concrete evidence that the loss of *Fah* is responsible for the *hsdr1* phenotype came with the targeted disruption of *Fah* exon 5, resulting in the same phenotype as the *hsdr1* deletion[37]. In addition, c^{14CoS} homozygous deletion mice carrying *Fah* transgenes are complemented for all aspects of the lethal *albino* phenotype[44]. These studies offer an explanation for the deletion phenotype that does not require the existence of a regulatory locus such as *hsdr1*. The evidence has proven that *hsdr1* and *Fah* are allelic and *Fah* deficiency is solely responsible for the disease phenotype.

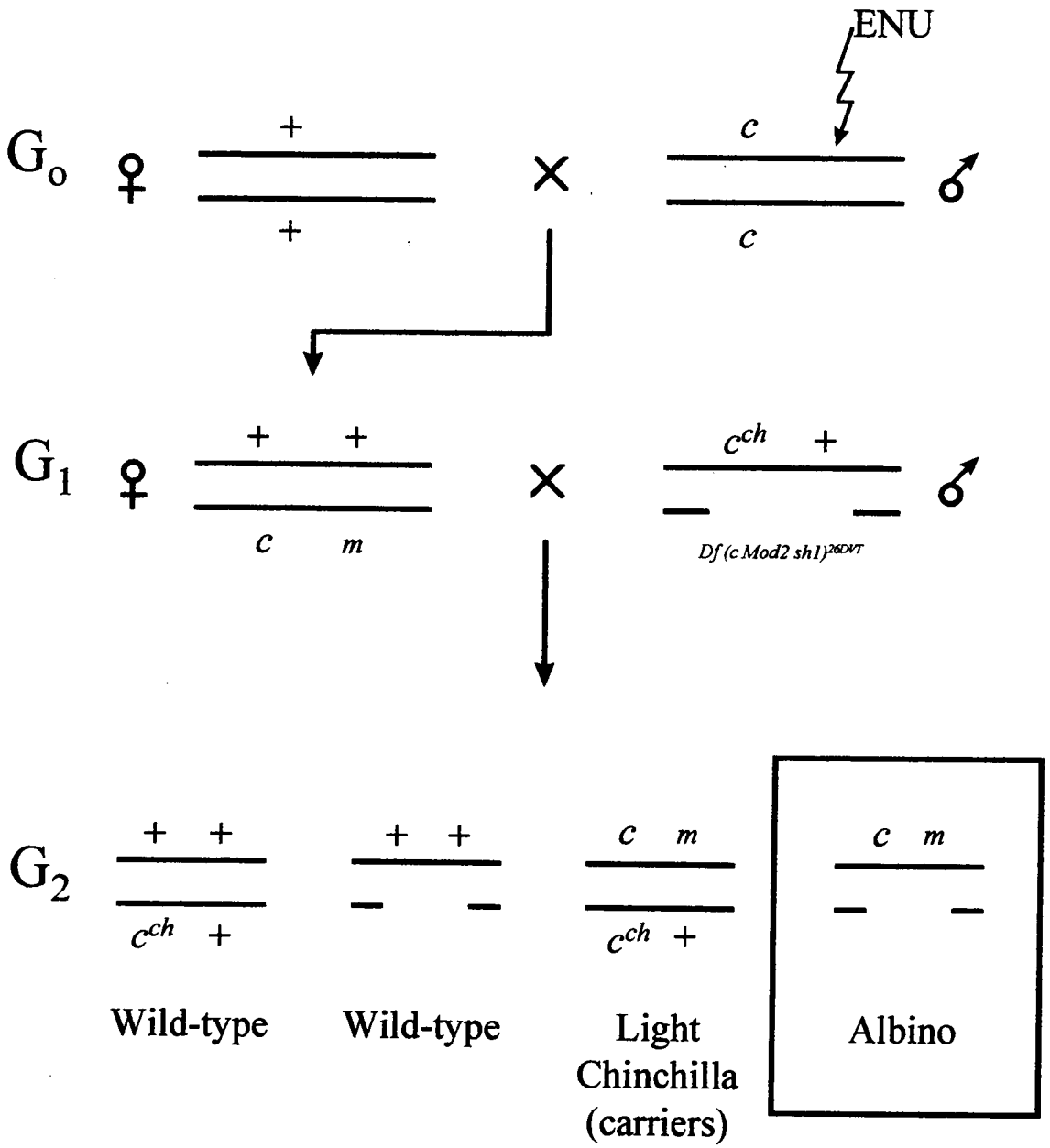
Many phenotypic similarities between human *FAH* and murine *Fah* deficiencies have been identified. Briefly both (1) suffer from tyrosinemia[38], (2) have increased levels of urinary amino acids that reflect liver and kidney dysfunction and impairment of amino

acid utilization[38], (3) have a reduction in activity of hepatic tyrosine aminotransferase and *S*-adenosylmethionine synthetase[34], and (4) have increased SA levels in serum[11,37]. In addition, affected mice have an increase in *gadd* gene expression[45] that suggests DNA damage, which relates to the chromosome breakage reported in human HT1 patients[3].

While murine *Fah* deficiency caused by deletion of the gene has many similarities to the HT1 disease in humans, the known human mutations are all point mutations within *FAH*. A more useful murine model of HT1 arose in experimental *N*-ethyl-*N*-nitrosourea (ENU)-saturation mutagenesis of a 6- to 11-cM region of mouse chromosome 7. This experiment was used to generate new recessive mutations that map to the *albino* region and thus further refine the functional map of the region[26]. The chemical ENU was chosen as the mutagen because it is known to be most effective in spermatogonial stem cells where it induces primarily point mutations[46,47].

Figure 1-3 depicts the breeding protocol used for the recovery of the ENU-induced mutations. Briefly, BALB/cRl (*albino*, *c* / *c*) males treated with ENU were mated to (C57Bl/10Rl x C3Hf/Rl) G_0 females (+ / +). Females carrying the mutagenized *albino* chromosome 7 were mated to males carrying the long *c* region deletion, c^{26DVT}. Hemizygous progeny that express albinism (the original recessive marker) would then express a new recessive mutation (*m*) located in the long *c*-region deletion. Newborn mutants lacking eye pigment can be distinguished from the pigmented *light chinchilla* carrier class (from which new lethal mutations can be recovered and propagated), as well as from the wild-type littermates. The saturation mutagenesis scheme resulted in the production of neonatally lethal mutants, that were mapped through trans

Figure 1-3. Breeding protocol for the detection of ENU-induced mutations in the *albino* region of mouse chromosome 7. Alleles of the *albino* locus, *c* (*albino*) and c^{ch} (*chinchilla*) are used as genetic recessive markers. The *Df (c Mod2 sh1)*^{26DVT} corresponds to the 6-11cM long c^{26DVT} deletion (refer to Fig. 1-4). The *m* represents the new ENU-induced mutation. The box denotes the G_2 *albino* test class, in which the new recessive mutations are evident and can be studied.

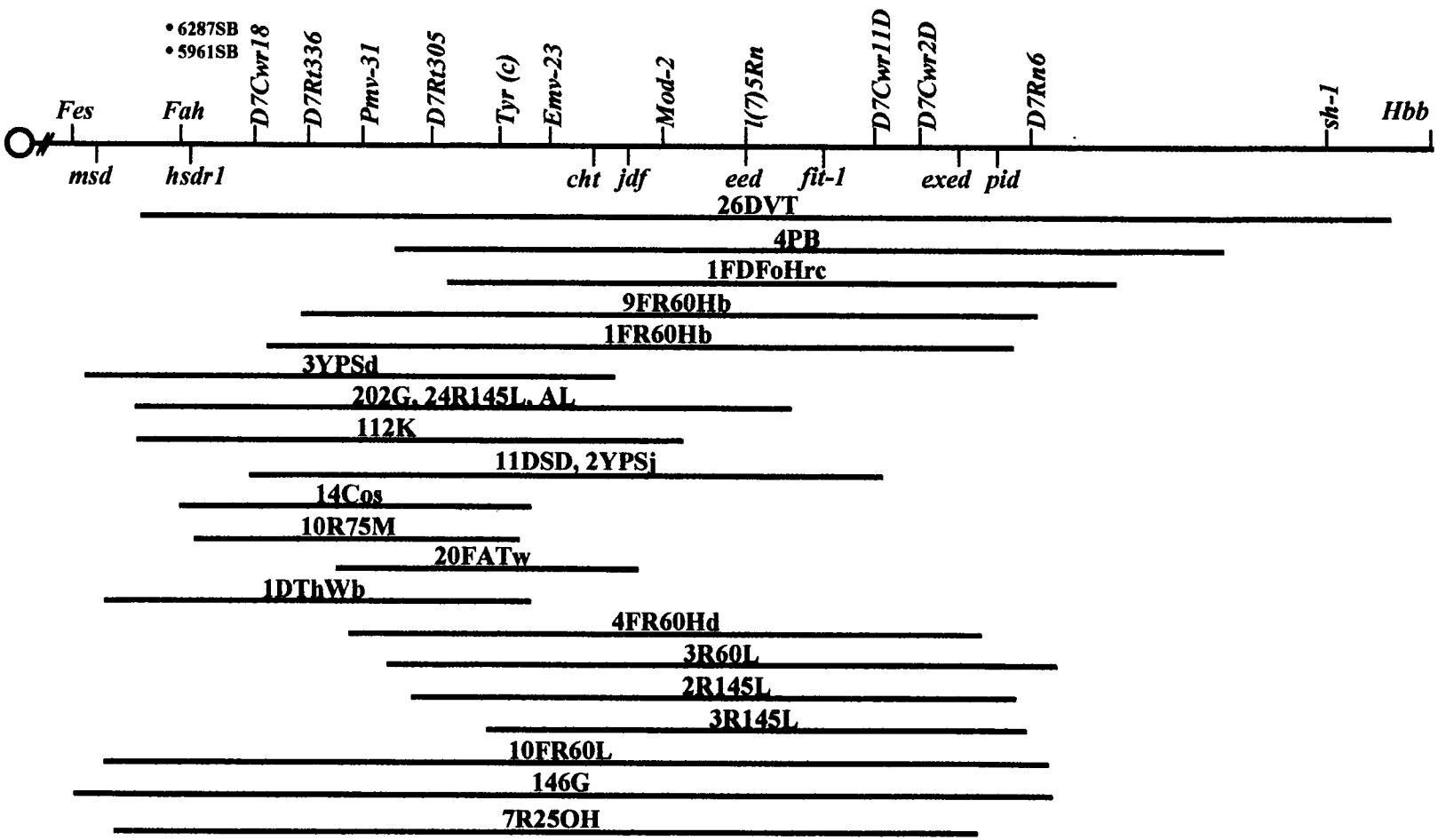

ENU
G$_o$
+
+
×
c
c
G$_1$
+ +
c m
×
c^{ch} +
Df (c Mod2 sh1)^{26DVT}
G$_2$
+ +
c^{ch} +
+ +
c m
c^{ch} +
c m
Wild-type
Wild-type
Light Chinchilla (carriers)
Albino

complementation crosses to mice carrying *c* deletions of varying length (Fig. 1-4). Two non-complementing neonatal lethal mutations, 5961SB and 6287SB were each complemented by deletions (c^{11DSD}, c^{4PB}) that do not cause the *Fah* deficiency phenotype[48-50] (E.M. Rinchik and D.A. Carpenter, unpubl.). However, neither of the two ENU-induced mutations was complemented by c^{14CoS}, c^{10R75M}, c^{112K}, c^{26DVT} or any other deletion known to extend into the *Fah* region (Fig. 1-4). Thus, at least a segment of the gene must map to the 315-kb region of non-overlap between the c^{14CoS} and c^{11DSD} deletions, the region known to encompass *Fah*. These data suggest that 5961SB and 6287SB are alleles at *Fah*, and may be designated fah^{5961SB} and fah^{6287SB}. Homozygotes for the fah^{5961SB} allele die during day one and fah^{6287SB} homozygotes die by the third week of life. Prior to this study, it was known that the ENU-induced mutations map to the region containing the *Fah* gene. This study establishes that mutations in the *Fah* gene are responsible for the neonatal lethal phenotype.

RESEARCH OBJECTIVES AND GENERAL OVERVIEW

To establish that mutations in *Fah* are responsible for the neonatal-lethal phenotype seen in the ENU-induced mutations 5961SB and 6287SB, it was necessary to locate the point mutation induced in each mutant. This identification of mutations was carried out by the complete sequencing of the *Fah* gene in each mutant, and comparing the sequences to the sequence of BALB/cRl, the inbred strain that was mutagenized by ENU in the saturation mutagenesis experiments. To prove that these mutations are indeed affecting *Fah* activity, we measured the levels of an abnormal tyrosine metabolite,

Figure 1-4. Complementation mapping of the ENU-induced neonatal lethal mutations, *fah*^{5961SB} and *fah*^{6287SB}, within the *albino* region of mouse chromosome 7. The placement of the ENU-induced lethal mutations on the map is based on complementation crosses with the indicated deletion chromosomes (E.M. Rinchik and D.A. Carpenter, unpubl.). Horizontal lines *beneath* the chromosome represent the subset of *c*-locus mutations that were used for the mapping of the mutations. The designation for each deletion is indicated directly *above* each line. Circle on the *left* represents the centromere. Genetic markers are shown *above* the chromosome in italics. Loci defined by complementation analysis of albino deletions are shown in italics *below* the chromosome. Detailed definitions and descriptions of DNA markers and loci have been described[52].


• 6287SB
• 5961SB
D7Cwr18
D7Rt336
Pmv-31
D7Rt305
Tyr (c)
Emv-23
Mod-2
l(7)5Rn
D7Cwr11D
D7Cwr2D
D7Rn6
sh-1
Hbb
Fes
Fah
msd
hsdr1
cht
jdf
eed
fit-1
exed
pid
26DVT
4PB
1FDFoHrc
9FR60Hb
1FR60Hb
3YPSd
202G, 24R145L, AL
112K
11DSD, 2YPSj
14Cos
10R75M
20FATw
1DThWb
4FR60Hd
3R60L
2R145L
3R145L
10FR60L
146G
7R25OH

SA, in urine using gas chromatography/mass spectrometry to provide identification and quantification of the metabolite in the complex profiles of urinary organic acids[51]. SA accumulates as a result of a deficiency in *Fah*, and its accumulation is diagnostic for HT1. The expression of *Fah* in the livers of the mutant mice was also determined by northern blot analysis to see if any alteration in amount and/or size of *Fah* mRNA exists as a result of the mutation. Sequence analysis, northern blot analysis, and SA identification were used to identify each mutation and to determine its effect on *Fah* mRNA expression and enzyme activity.

The thesis consists of one journal-style paper in part 2:

Part 2 is "Point mutations in the murine *Fah* gene: Animal models for the human genetic disorder hereditary tyrosinemia type 1", which has been submitted for publication.

Appendix A contains supplementary data that is discussed but not presented in Part 2.

REFERENCES

1. Goldsmith, L.A., Laberge, C. Tyrosinemia and related disorders. *The metabolic basis of inherited disease* (McGraw-Hill, New York, 6th ed. Vol. 1547-562, 1989).

2. Kvittingen, E.A. Hereditary tyrosinemia type 1 - an overview. *Scand. J. Clin. Lab. Invest.* **46** (184), 27-34 (1986).

3. Gilbert-Barness, E., Barness, L.A., Meisner, L.F. Chromosomal instability in hereditary tyrosinemia type I. *Pediatr. Pathol.* **10** (1-2), 243-252 (1990).

4. Tanguay, R.M. *et al.* Different molecular basis for fumarylacetoacetate hydrolase deficiency in two clinical forms of hereditary tyrosinemia (type 1). *Am. J. Hum. Genet.* **47**, 308-316 (1990).

5. Phaneuf, D. *et al.* Type 1 hereditary tyrosinemia: evidence for molecular heterogeneity and identification of a causal mutation in a French Canadian patient. *J. Clin. Invest.* **90**, 1185-1192 (1992).

6. Berger, R., van Faassen, H., Smith, G.P.A. Biochemical studies on the enzymatic deficiencies in hereditary tyrosinemia. *Clinica Chimica Acta* **134**, 129-141 (1983).

7. Overturf, K. *et al.* Hepatocytes corrected by gene therapy are selected *in vivo* in a murine model of hereditary tyrosinemia type 1. *Nature Genet.* **12**, 266-273 (1996).

8. Sassa, A., Kappas, A. Hereditary tyrosinemia and the heme biosynthetic pathway. *J. Clin. Invest.* **71** (3), 625-634 (1983).

9. Manabe, S., Sassa, S., Kappas, A. Hereditary tyrosinemia. *J. Exp. Med.* **162** (3), 1060-1074 (1985).

10. Pettit, B.R., MacKenzie, F., King, G.S. The antenatal diagnosis and aid to the management of hereditary tyrosinaemia by use of a specific and sensitive GC-MS assay for succinylacetone. *J. Inher. Metab. Dis.* **7** (2), 135-136 (1984).

11. Grenier, A., Lescault, A., Laberge, C., Gagne, R., Mamer, O. Detection of succinylacetone and the use of its measurement in mass screening for hereditary tyrosinemia. *Clinica Chimica Acta* **123**, 93-99 (1982).

12. Linstedt, S., Holme, E., Lock, E.A., Hjalmarson, O., Strandvik, B. Treatment of hereditary tyrosinaemia type 1 by inhibition of 4-hydroxyphenylpyruvate dioxygenase. *Lancet* **340**, 813-817 (1992).

13. Kvittingen, E.A., Brodtkorb, E. The pre- and post-natal diagnosis of tyrosinemia type 1 and the detection of the carrier state by assay of fumarylacetoacetase. *Scand. J.*

Clin. Lab. Invest. **46** (184), 35-40 (1986).

14. Rootwelt, H. *et al.* The human fumarylacetoacetase gene: characterization of restriction fragment length polymorphisms and identification of haplotypes in tyrosinemia type 1 and pseudodeficiency. *Hum. Genet.* **89**, 229-223 (1992).

15. Labelle, Y., Phaneuf, D., Leclerc, B., Tanguay, R.M. Characterization of the human fumarylacetoacetate hydrolase gene and identification of a missense mutation abolishing enzymatic activity. *Hum. Mol. Genet.* **2** (7), 941-946 (1993).

16. Rootwelt, H. *et al.* Two missense mutations causing tyrosinemia type 1 with presence and absence of immunoreactive fumarylacetoacetate. *Hum. Genet.* **93**, 615-619 (1994).

17. St-Louis, M. *et al.* Identification of a stop mutation in five Finnish patients suffering from hereditary tyrosinemia type 1. *Hum. Mol. Genet.* **3** (1), 69-72 (1994).

18. St-Louis, M. *et al.* Two novel mutations involved in hereditary tyrosinemia type 1. *Hum. Mol. Genet.* **4** (2), 319-320 (1995).

19. Ploos van Amstel, J.K. *et al.* Hereditary tyrosinemia type 1: novel missense, nonsense and splice consensus mutations in the human fumarylacetoacetate hydrolase gene; variability of the genotype-phenotype relationship. *Hum. Genet.* **97**, 51-59 (1996).

20. Timmers, C., Grompe, M. Six novel mutations in the fumarylacetoacetate hydrolase gene of patients with hereditary tyrosinemia type 1. *Hum. Mut.* **7**, 367-369 (1996).

21. Kvittingen, E.A., Rootwelt, H., van Dam, T., van Faassen, H., Berger, R. Hereditary tyrosinemia type I: lack of correlation between clinical findings and amount of immunoreactive fumarylacetoacetase protein. *Pediatr. Res.* **31** (1), 43-46 (1992).

22. Berger, R., van Faassen, H., Taanman, J.W., De Vries, H., Agsteribbe, E. Type 1 tyrosinemia: lack of immunologically detectable fumarylacetoacetase enzyme protein in tissues and cell extracts. *Pediatr. Res.* **22** (4), 394-398 (1987).

23. Phaneuf, D. *et al.* Cloning and expression of the cDNA encoding human fumarylacetoacetate hydrolase, the enzyme deficient in hereditary tyrosinemia: assignment of the gene to chromosome 15. *Am. J. Hum. Genet.* **4**, 525-535 (1991).

24. Awata, H. *et al.* Structural organization and analysis of the human fumarylacetoacetate hydrolase gene in tyrosinemia type 1. *Biochimica et Biophysica Acta* **1226**, 168-172 (1994).

25. Russell, L.B., Montgomery, C.S., Raymer, G.D. Analysis of the albino-locus region of the mouse: IV. characterization of 34 deficiencies. *Genetics* **100**, 427-453 (1982).

26. Rinchik, E.M., Russell, L.B. Germ-line deletion mutations in the mouse: tools for intensive functional and physical mapping of regions of the mammalian genome. *Genome Analysis* (Vol 1: Genetic and Physical Mapping. Cold Spring Harbor Laboratory Press, 1990).

27. Russell, W.L. X-ray-induced mutations in mice. *Cold Spring Harbor Symp. Quant. Biol.* **16**, 327 (1951).

28. Russell, W.L. Reminiscences of a mouse specific-locus test addict. *Envir. Mol. Mut.* **14** (16), 16-22 (1989).

29. Russell, W.L. *et al.* Specific-locus test shows ethylnitrosourea to be the most potent mutagen in the mouse. *Proc. Natl. Acad. Sci.* **76** (11), 5818-5819 (1979).

30. Gluecksohn-Waelsch, S. Genetic control of morphogenetic and biochemical differentiation: lethal albino deletions in the mouse. *Cell* **16**, 225-237 (1979).

31. Schmid, W., Muller, G., Schutz, G., Gluecksohn-Waelsch, S. Deletions near the albino locus on chromosome 7 of the mouse affect the level of tyrosine aminotransferase mRNA. *Proc. Natl. Acad. Sci.* **82**, 2866-2869 (1985).

32. Ruppert, S. *et al.* Two genetically defined trans-acting loci coordinately regulate overlapping sets of liver-specific genes. *Cell* **61**, 895-904 (1990).

33. DeFranco, D. *et al.* The glucocorticoid hormone signal transduction pathway in mice homozygous for chromosomal deletions causing failure of cell type-specific inducible gene expression. *Proc. Natl. Acad. Sci.* **88**, 5607-5610 (1991).

34. Ruppert, S. *et al.* Deficiency of an enzyme of tyrosine metabolism underlies altered gene expression in newborn liver of lethal albino mice. *Genes Dev.* **6**, 1430-1443 (1992).

35. Gluecksohn-Waelsch, S. Regulatory genes in development. *TIG* **3** (5), 123-127 (1987).

36. Petersen, D.D. *et al.* Marked increases in hepatic NAD(P)H:oxidoreductase gene transcription and mRNA levels correlated with a mouse chromosome 7 deletion. *Proc. Natl. Acad. Sci.* **86**, 6699-6703 (1989).

37. Grompe, M. *et al.* Loss of fumarylacetoacetate hydrolase is responsible for the neonatal hepatic dysfunction phenotype of lethal albino mice. *Genes Dev.* **7**, 2298-2307 (1993).

38. Grompe, M. Pharmacological correction of neonatal lethal hepatic dysfunction in a

murine model of hereditary tyrosinemia type 1. *Nature Genet.* **10**, 453-460 (1995).

39. Kelsey, G., Schutz, G. Lessons from lethal albino mice. *Curr. Opin. Genet. Dev.* **3**, 259-264 (1993).

40. Niswander, L. *et al.* Molecular mapping of albino deletions associated with early embryonic lethality in the mouse. *Genomics* **9**, 162-169 (1991).

41. Kelsey, G. *et al.* Physical mapping of the albino-deletion complex in the mouse to localize *alf/hsdr-1*, a locus required for neonatal survival. *Genomics* **14**, 275-287 (1992).

42. Schedl, A. *et al.* Chromosome jumping from flanking markers defines the minimal region for *alf/hsdr-1* within the albino-deletion complex. *Genomics* **14**, 288-297 (1992).

43. Klebig, M.L., Russell, L.B., Rinchik, E.M. Murine fumarylacetoacetate hydrolase (*Fah*) gene is disrupted by a neonatally lethal albino deletion that defines the hepatocyte-specific developmental regulation 1 (*hsdr-1*) locus. *Proc. Natl. Acad. Sci.* **89**, 1363-1367 (1992).

44. Kelsey, G. *et al.* Rescue of mice homozygous for lethal albino deletions: implications for an animal model for the human liver disease tyrosinemia type 1. *Genes Dev.* **7**, 2285-2297 (1993).

45. McInnes, R.R., Byers, P.H. Biochemical genetics: examples of life after cloning. *Curr. Opin. Genet. Dev.* **3**, 475-483 (1993).

46. Russell, L.B., Russell, W.L., Rinchik, E.M., Hunsicker, P.R. Factors affecting the nature of induced mutations. *Banbury Rep.* **34**, 271-289 (1990).

47. Russell, L.B. Role of mouse germ-cell mutagenesis in understanding genetic risk and in generation mutations that are prime tools for studies in modern biology. *Envir. Mol. Mut.* **23** (24), 23-29 (1994).

48. Rinchik, E.M., Carpenter, D.A., Selby, P.B. A strategy for fine-structure functional analysis of a 6- to 11-centimorgan region of mouse chromosome 7 by high-efficiency mutagenesis. *Proc. Natl. Acad. Sci.* **87**, 896-900 (1990).

49. Rinchik, E.M., Carpenter, D.A. *N*-ethyl-*N*-nitrosourea-induced prenatally lethal mutations define at least two complementation groups within the embryonic ectoderm development (*eed*) locus in mouse chromosome 7. *Mammal. Genome* **4**, 349-353 (1993).

50. Holdener, B.C. *et al.* Physical location of *eed*: a region of mouse chromosome 7

required for gastrulation. *Genomics* **27**, 447-456 (1995).

51. Schierbeek, H., Berger, R. Determination of succinylacetone and succinylacetoacetate in physiological samples as the common product 5(3)-methyl-3(5)-isoxazole propionic acid using an isotope dilution method and mass spectrometry. *Clinica Chimica Acta* **184**, 243-250 (1989).

Rinchik, E.M. *et al.* Mouse chromosome 7. *Mammal. Genome* **3**, S104-S120 (1992).

Part 2

Point Mutations in the Murine *Fah* Gene: Animal Models for the Human Genetic Disorder Hereditary Tyrosinemia Type 1

ABSTRACT

Hereditary tyrosinemia type 1 (HT1) is a severe autosomal recessive metabolic disease, associated with point mutations in the human fumarylacetoacetate hydrolase (*FAH*) gene that cause disruption of tyrosine catabolism. The acute form results in death during the first months of life due to hepatic failure, while the chronic form leads to gradual liver disease development often accompanied by renal dysfunction, childhood rickets, neurological crisis, and hepatocellular carcinoma. In the mouse, *Fah* maps near the *albino* (*c*) locus in chromosome 7. Mice homozygous for specific deletions around *c* that include *Fah* die perinatally as a result of liver dysfunction and exhibit a complex syndrome characterized by structural abnormalities of the liver and kidney, and alterations in gene expression. Here we report that two mutations induced by *N*-ethyl-*N*-nitrosourea (ENU) and mapped near *c* are alleles of *Fah*. The fah^{6287SB} allele is a missense mutation in exon 6 causing a reduction of *Fah* mRNA levels, and fah^{5961SB} is a splice mutation causing loss of exon 7, a subsequent frameshift in the resulting mRNA, and a severe reduction of *Fah* mRNA levels. Increased levels of the diagnostic metabolite succinylacetone in the urine of the fah^{6287SB} and fah^{5961SB} mutants indicates that the mutations cause a decrease in Fah enzymatic activity. Thus, the neonatal phenotype present in both mutants is due to a deficiency in Fah caused by a point mutation, and we propose fah^{5961SB} and fah^{6287SB} as mouse models for the acute and chronic forms of HT1, respectively.

INTRODUCTION

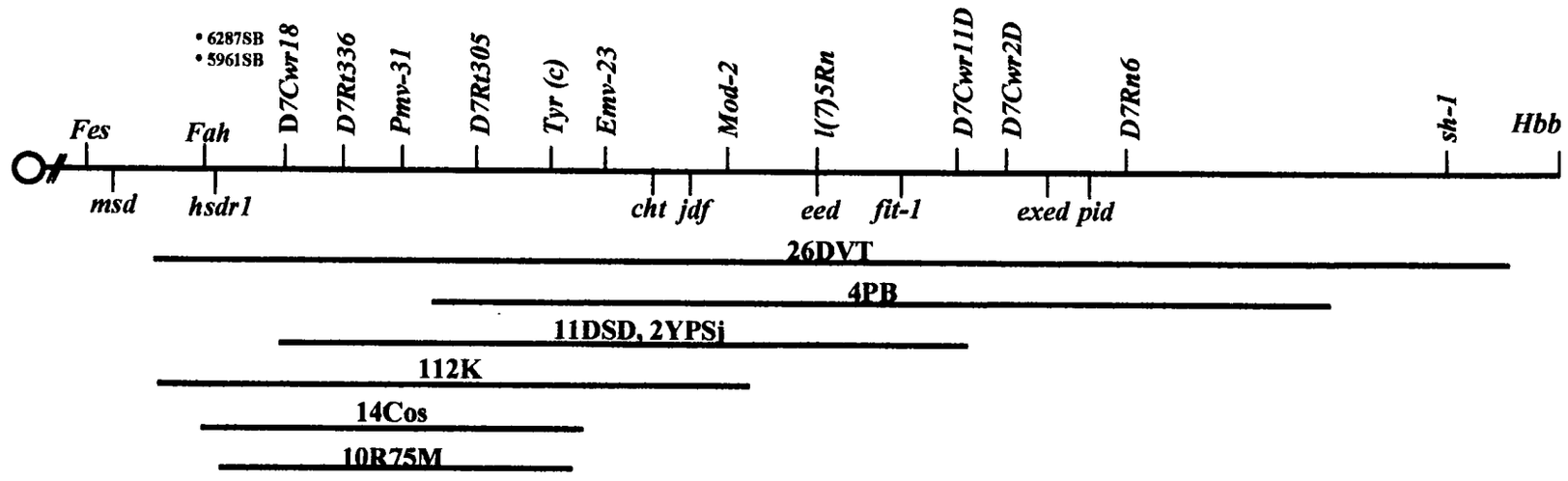
Hereditary tyrosinemia type 1 (HT1) is an autosomal recessive disease caused by a deficiency of fumarylacetoacetate hydrolase (FAH), the last enzyme in the catabolic pathway of tyrosine[1]. FAH deficiency results in the accumulation in the liver and kidney of fumarylacetoacetate (FAA), maleylacetoacetate (MAA), and succinylacetone (SA), which are believed to be responsible for certain pathological aspects of the disorder[2,3]. There are two major clinical forms of the disease, acute and chronic, which can be distinguished on the basis of the residual amount of liver FAH activity[4,5]. The metabolic disorder is clinically heterogeneous[1,6]. In the acute form, symptoms appear during the first months of life and death due to hepatic failure usually occurs during the first year. The chronic form results in a gradual liver disease in which individuals develop childhood rickets, suffer from renal tubule defects, and often develop hepatocarcinoma in their teens. Biochemically, the disease is characterized by the accumulation of tyrosine, tyrosine metabolites, methionine, and SA in serum and/or urine[1]. SA accumulation is unique to FAH deficiency[6,7] and its presence is diagnostic for the disease[2,8,9]. The disease has a worldwide distribution with a high incidence in the French Canadian and Scandinavian populations[1,6].

The *FAH* gene is located on chromosome 15q23-q25[10]. At least 26 different mutations in *FAH* have been identified in HT1 patients, including missense, nonsense and splice consensus site mutations[5,11-17]. Likewise, it has been shown that the *hsdr1* (*hepatocyte-specific developmental regulation-1*)[18] phenotype in mice results from the deletion or targeted disruption of the *Fah* gene on mouse chromosome 7[19-21].

The mouse *hsdr1* locus is defined by 37 overlapping radiation-induced deletions that remove the *c* (*albino*) locus and surrounding regions of mouse chromosome 7. The *albino*-deletion complex was derived in specific-locus mutagenesis experiments where the *c* locus served as one of seven recessive marker loci[22]. Each of the loci was originally selected for easy visible detection in the homozygous state and a set of overlapping radiation-induced deletions is associated with each specific locus[23]. The *albino* deletion complex is one of the best characterized of the specific-locus deletion complexes. Embryological and complementation analysis classified these *c* deletions into 13 groups that define at least 6 loci necessary for either pre- or postnatal development[18,23-25]. The locus *hsdr-1* was found to be required for postnatal survival, since mice homozygous for certain deletions (ie. c^{14CoS}, c^{10R75M}, Fig. 2-1) die shortly after birth. The mice die as a result of hypoglycemia due to a failure to express in the liver and kidneys high, neonatal levels of glucose-6 phosphatase and other enzymes associated with gluconeogenesis[18]. The deficiency also causes structural abnormalities of the liver and kidney, and hepatocytes and proximal convoluted tubule cells have reduced levels of many enzymes and proteins, and increased transcription of enzymes involved in defending against oxidative stress and DNA damage[18,20,21,26,27]. It was proposed that *hsdr1* harbors regulatory gene(s) required for the perinatal activation of a set of hormone-inducible structural genes in the liver and kidney[18,28].

It was found through complementation analysis using overlapping deletions (ie., c^{11DSD}, c^{14CoS}, c^{112K}, c^{4PB}, Fig. 2-1) that the c^{11DSD} deletion complements the c^{14CoS} disease phenotype[25]. The minimal region for *hsdr1* was then further defined to the 315-kb

Figure 2-1. Complementation mapping of two ENU-induced neonatal lethal mutations within the *c* region of mouse chromosome 7. Horizontal lines *beneath* the chromosome represent the subset of *c*-locus mutations that were used for the mapping of the mutations. The designation for each deletion is indicated directly *above* each line. Circle on the *left* represents the centromere. Genetic markers are shown *above* the chromosome in italics. Loci defined by complementation analysis of *albino* deletions are shown in italics *below* the chromosome. Detailed definitions and descriptions of DNA markers and loci have been described[48]. The proximal breakpoints of the c^{14CoS} and c^{11DSD} deletions flank the *Fah* region. The proximal breakpoint of the c^{10R75M} deletion maps <1 kilobase 5' to the start of *Fah* transcription and is believed to remove sequences essential for expression of Fah^{20}.


• 6287SB
• 5961SB
Fes
Fah
D7Cwr18
D7Rt336
Pmv-31
D7Rt305
Tyr (c)
Emv-23
Mod-2
l(7)5Rn
D7Cwr11D
D7Cwr2D
D7Rn6
sh-1
Hbb
msd
hsdr1
cht
jdf
eed
fit-1
exed
pid
26DVT
4PB
11DSD, 2YPSj
112K
14Cos
10R75M

interval at the proximal end of the c^{14CoS} deletion from the identification of the deletion breakpoints that flank the interval[20,29-31]. The gene encoding fumarylacetoacetate hydrolase (*Fah*) was shown to be disrupted by the c^{14CoS} deletion and was proposed as a candidate for *hsdr1*[19,20].

Much evidence has been presented indicating that loss of the *Fah* gene in the deletion mutants can account for all aspects of the *hsdr1* phenotype[20,21,32]. Briefly, changes in gene expression were mimicked in hepatocytes treated with homogentisic acid (precursor of MAA and FAA)[20], targeted disruption of *Fah* exon 5 results in the same phenotype as the *hsdr1* deletion[21], and mice homozygous for c^{14CoS} and carrying *Fah* transgenes are complemented for all aspects of the lethal *albino* phenotype[32]. These studies offer an explanation for the deletion phenotype that does not require the existence of a regulatory locus such as *hsdr1*, and prove that *hsdr1* and *Fah* are allelic and that Fah deficiency is solely responsible for the disease phenotype.

Whereas the *Fah* null allele, in mice carrying radiation-induced deletions, causes early lethality (within hours of birth), the known cases of human HT1 result from point mutations within *FAH*. A more suitable model for human HT1 may be seen in neonatally lethal mutations near *c* generated in a saturation mutagenesis experiment of a 6- to 11-cM region of mouse chromosome 7 with *N*-ethyl-*N*-nitrosourea (ENU). These lethal mutations were mapped through trans complementation crosses to mice carrying *c* deletions and two non-complementing neonatal lethal mutations (*5961SB* and *6287SB*) failed to complement c^{14CoS}, c^{10R75M}, c^{112K}, c^{26DVT} or any other deletion known to extend into the *Fah* region[33-35] (Fig. 2-1, E.M. Rinchik and D.A. Carpenter, unpubl.). However,

c^{4PB} and c^{11DSD} both complement each of the mutations for neonatal lethality, mapping the point mutations to the 315-kb region of non-overlap between the proximal ends of the c^{14CoS} and c^{11DSD} deletions, the region known to include *Fah* (E.M. Rinchik and D.A. Carpenter, unpubl.). These data suggest that *5961SB* and *6287SB* are alleles at *Fah*, and may be designated as fah^{5961SB} and fah^{6287SB}. Homozygosity for fah^{5961SB} results in death during day one, while homozygosity for fah^{6287SB} causes death by the third week of life.

We report here that fah^{6287SB} is a missense mutation in exon 6 of the *Fah* gene and that fah^{5961SB} harbors a splice mutation causing the loss of exon 7 and a subsequent frameshift in the resulting mRNA. mRNAs for both alleles are expressed at reduced levels in the livers of affected mice, the fah^{5961SB} mutation causing the more severe reduction. We also report the increased levels of SA, a metabolic abnormality specific for *Fah* deficiency, in the urine of the fah^{6287SB} and fah^{5961SB} mutants, confirming that the mutations identified here cause a decrease in Fah enzymatic activity. Thus, the neonatal phenotype present in both mutants is due to a deficiency in *Fah* caused by a point mutation, establishing fah^{5961SB} and fah^{6287SB} as mouse models for the acute and chronic human forms of HT1, respectively.

RESULTS

Isolation of the *Fah* cDNAs and Identification of Point Mutations. To examine *albino* mutant strains for mutations affecting the *Fah* open reading frame, cDNAs were amplified by RT-PCR. The amplified fragments were analyzed by electrophoresis; all lanes containing BALB/cRl or *fah*^{6287SB} cDNA showed fragments of the expected size, whereas the *fah*^{5961SB} cDNA showed an abnormal fragment size of reduced (~100bp) length (Fig. A-1).

All exons were screened for point mutations by direct sequencing of two independently amplified fragments. Wild-type (BALB/cRl) cDNA sequence was identical to that previously reported for a full *Fah* mouse cDNA clone (Klebig *et al.*, 1992), including an open reading frame of 1257 bp coding for 419 amino acids starting from the first ATG at position 1 and ending at the TGA at position 1258. Direct sequencing of the *fah*^{6287SB} cDNA revealed an A→G transition causing a missense mutation in nucleotide position 602 (Fig. 2-2), introducing glycine in place of glutamic acid in amino acid position 201 (E201G). Direct sequencing of the *fah*^{5961SB} allele cDNA product revealed that nucleotides 607-706 that constitute the 7th exon of murine FAH are deleted (607d100, Fig. 2-2). The cDNA is altered in a manner consistent with changed patterns of RNA splicing (Fig. 2-3). The deletion of exon 7 resulted in a frameshift and subsequently the introduction of a premature stop codon at amino acid position 270, the previous location of amino acids 303/304 in exon 9. The exact genomic location of the mutation is under investigation but is believed to be present in a consensus sequence required for correct pre-mRNA splicing.

Figure 2-2. Nucleotide sequences of **exons 6, 7 and 8** of control BALB/cRl, mutant *fah*^{6286SB}, and mutant *fah*^{5961SB}. Line **A**, nucleotide sequence of murine BALB/cRl cDNA. Line **B**, nucleotide sequence of the murine *fah*^{6287SB} cDNA. Line **C**, nucleotide sequence of the murine *fah*^{5961SB} cDNA. Numbers to *left* refer to nucleotide residues from the initiating nucleotides. Mutant *fah*^{6287SB} has a point mutation at nucleotide 602, as indicated by the **G** at this position in line **B**. The dashes (--) indicate the nucleotides missing in the murine *fah*^{5961SB} sequence.

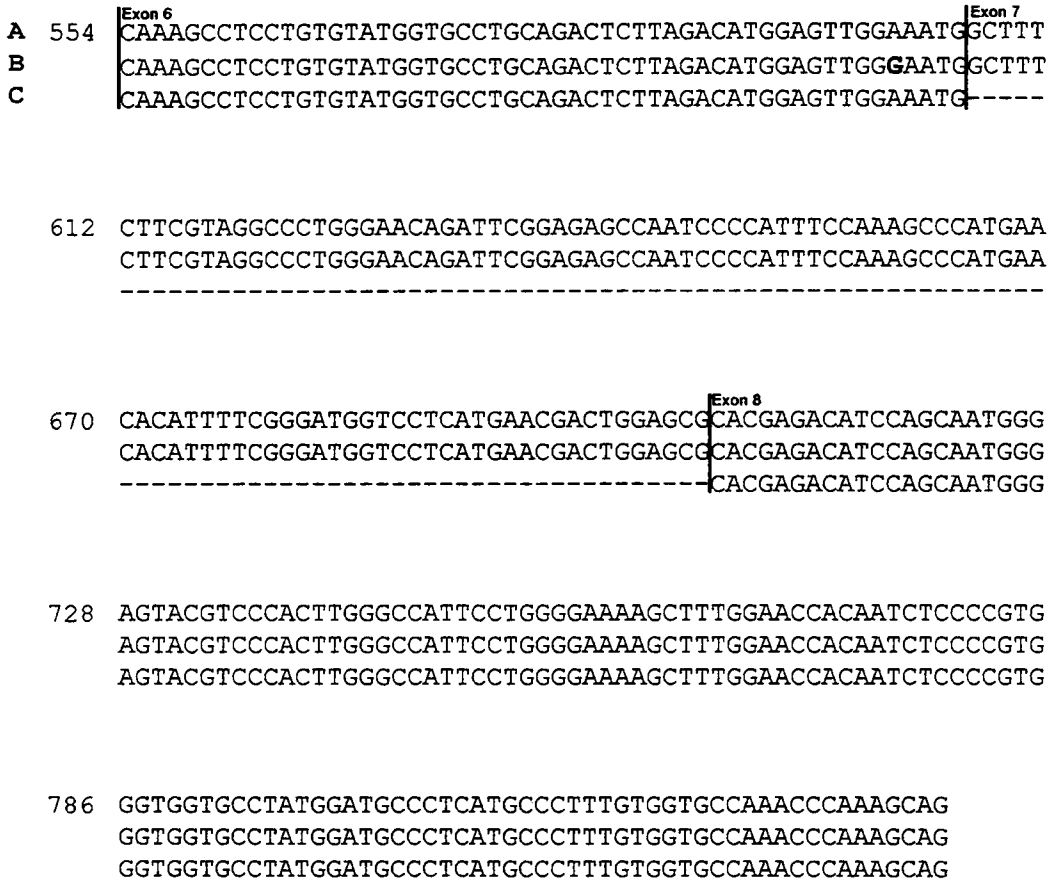
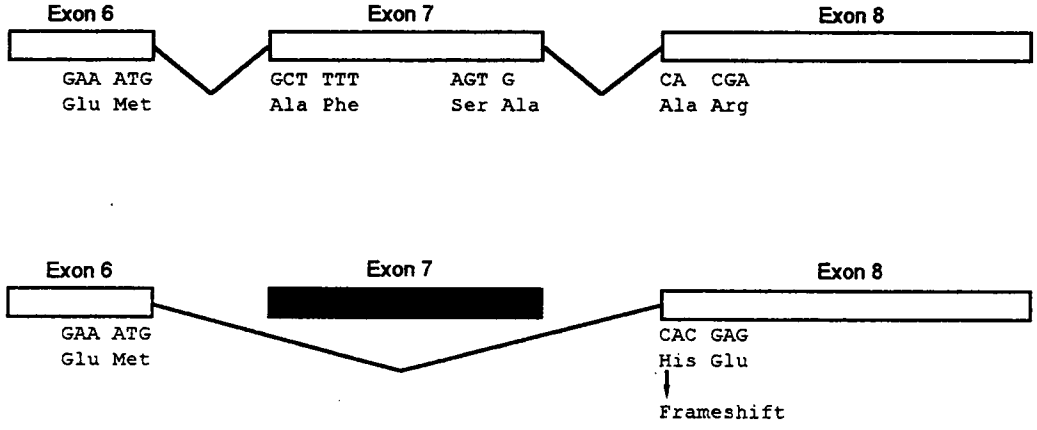

Exon 6
Exon 7
A 554 CAAAGCCTCCTGTGTATGGTGCCTGCAGACTCTTAGACATGGAGTTGGAAATGGCTTT
B CAAAGCCTCCTGTGTATGGTGCCTGCAGACTCTTAGACATGGAGTTGGGAATGGCTTT
C CAAAGCCTCCTGTGTATGGTGCCTGCAGACTCTTAGACATGGAGTTGGAAATG-----
612 CTTCGTAGGCCCTGGGAACAGATTCGGAGAGCCAATCCCCATTTCCAAAGCCCATGAA
CTTCGTAGGCCCTGGGAACAGATTCGGAGAGCCAATCCCCATTTCCAAAGCCCATGAA
Exon 8
670 CACATTTTCGGGATGGTCCTCATGAACGACTGGAGCGCACGAGACATCCAGCAATGGG
CACATTTTCGGGATGGTCCTCATGAACGACTGGAGCGCACGAGACATCCAGCAATGGG
CACGAGACATCCAGCAATGGG
728 AGTACGTCCCACTTGGGCCATTCCTGGGGAAAAGCTTTGGAACCACAATCTCCCCGTG
AGTACGTCCCACTTGGGCCATTCCTGGGGAAAAGCTTTGGAACCACAATCTCCCCGTG
AGTACGTCCCACTTGGGCCATTCCTGGGGAAAAGCTTTGGAACCACAATCTCCCCGTG
786 GGTGGTGCCTATGGATGCCCTCATGCCCTTTGTGGTGCCAAACCCAAAGCAG
GGTGGTGCCTATGGATGCCCTCATGCCCTTTGTGGTGCCAAACCCAAAGCAG
GGTGGTGCCTATGGATGCCCTCATGCCCTTTGTGGTGCCAAACCCAAAGCAG

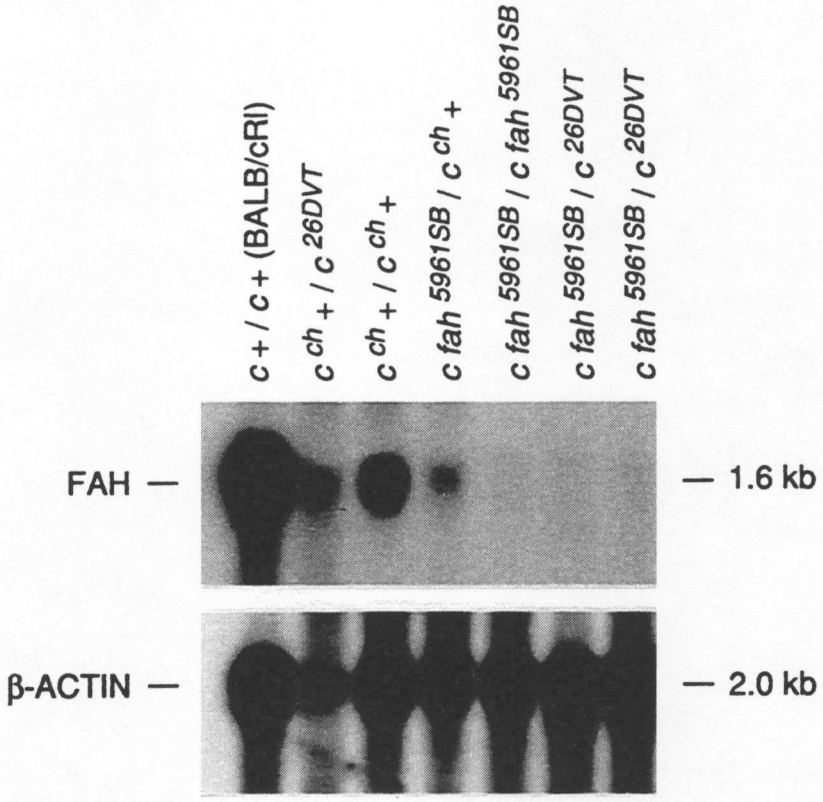
Figure 2-3. Schematic representation of the *fah*^{5961SB} mutation, and its effect on the processing of the *Fah* mRNA. The mutation results in an altered pattern of mRNA splicing, causing the loss of the exon 7 sequence from the murine *Fah* mRNA and a subsequent shift in the reading frame to introduce a premature stop codon in exon 9.


Exon 6
Exon 7
Exon 8
GAA ATG
Glu Met
GCT TTT
Ala Phe
AGT G
Ser Ala
CA CGA
Ala Arg
Exon 6
Exon 7
Exon 8
GAA ATG
Glu Met
CAC GAG
His Glu
Frameshift

Expression of the Normal *Fah* mRNA in the Livers of *fah*^{5961SB} and *fah*^{6287SB} Mice. Northern blot hybridization to the *Fah* cDNA was utilized to determine if there was any significant alteration in the amount and/or size of the *Fah* mRNA in livers of the mutant mice. In control livers there are two predominant mRNA species that migrate at ~1.6kb (Fig. 2-4, lanes 1 and 3) and ~3.5kb (data not shown). Homozygous *fah*^{5961SB} mutants (Fig. 2-4, lane 5) and hemizygous *fah*^{5961SB} mutants (Fig. 2-4, lanes 6-7) had mRNA of equal size but greatly decreased amounts compared to controls, when correlated to actin mRNA loading. Heterozygous carriers of the *fah*^{5961SB} (Fig. 2-4, lane 4) mutation appeared to have intermediate mRNA levels compared to control and mutant levels. *Fah* mRNA of normal size was present in reduced amounts in the livers of the *fah*^{6287SB}, mutants but was not as severely reduced as in the *fah*^{5961SB} mutation (Fig. A-2).

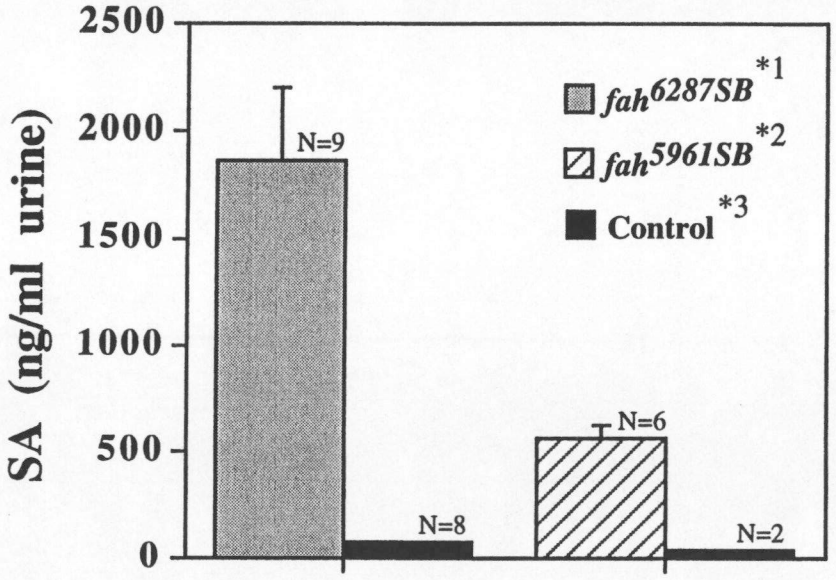
Neonatal Death of *fah*^{5961SB} and *fah*^{6287SB} Homozygotes and Hemizygotes. Males heterozygous for either the *fah*^{5961SB} or *fah*^{6287SB} mutation were bred to females heterozygotes (*c* m / c^{ch} +) or to females carrying the 26DVT deletion (c^{ch} + / c^{26DVT}) and litters containing *albino* offspring were observed daily. No obvious differences in morphology or size were noted immediately after birth and all pups appeared healthy. In *fah*^{5961SB} litters, however, dead *albino* pups (identified by lack of eye pigment) were found after about 12 hours, with no *fah*^{5961SB} mutants surviving past 24 hours after birth. In *fah*^{6287SB} litters, *albino* pups died 10-20 days after birth, with the majority dying at days 12-14. No *fah*^{6287SB} *albino* mutants survived past 1 month.

Figure 2-4. Northern Blot analysis of the *Fah* gene. Expression of *Fah* mRNA in livers from wild-type mice and *fah*^{5961SB} mutants with the splicing mutation is shown. The genotype of the animals is given at the *top* and the probe used is given to the *left* of each blot. Each lane contains 10μg of total liver RNA probed with a ^{32}P-labelled *Fah* cDNA and reprobed with a β-actin probe. Sizes (in kb) of the major transcript identified by each probe are indicated.


c +/c + (BALB/cRl)
c ch +/c 26DVT
c ch +/c ch +
c fah 5961SB/c ch +
c fah 5961SB/c fah 5961SB
c fah 5961SB/c 26DVT
c fah 5961SB/c 26DVT
FAH —
— 1.6 kb
β-ACTIN —
— 2.0 kb

Biochemical Abnormality in *fah*^{5961SB} and *fah*^{6287SB} Mutant Mice. Succinylacetone concentrations above normal levels is a specific abnormality caused by FAH deficiency[6,7]. To detect this compound, organic acids were extracted from urine and analyzed quantitatively by gas chromatography / mass spectrometry. SA levels in *fah*^{5961SB} and *fah*^{6287SB} hemizygous mutants were compared to that of control mice of the same age, Fig. 2-5 shows average SA values pooled by mutation. From ages 2-11, *fah*^{6287SB} mice (*c fah*^{6287SB} / *c*^{26DVT}) had significantly greater SA concentrations compared to same day controls (all of genotype *c*^{ch} + / *c*^{ch} +, except age 2 control could also be of genotype *c fah*^{6287SB} / *c*^{ch} + or *c*^{ch} + / *c*^{26DVT}) . The *fah*^{6287SB} hemizygotes had SA levels of 484 - 3138 ng/ml (age 2, 484 ng/ml; age 7, 3138 ng/ml; age 9, 2060 ng/ml avg.; age 11, 1714 ng/ml avg.). SA values in wild-type urine ranged from undetectable to 170 ng/ml (age 2, 50 ng/ml; age 7, undetectable; age 9, 89 ng/ml; age 11, 80 ng/ml avg.). In *fah*^{5961SB} hemizygotes at age 0 (*c fah*^{5961SB} / *c*^{26DVT}) SA levels ranged from 347 - 837 ng/ml (552 ng/ml avg.), and controls at age 0 (*c*^{ch} + / *c*^{ch} +, *c fah*^{5961SB} / *c*^{ch} + or *c*^{ch} + / *c*^{26DVT}) averaged 36 ng/ml. SA levels in human HT1 patients are of the same order of magnitude (.19 - 253 μg/ml)[36]. There is no significant difference in SA levels between adult controls (76ng/ml avg.) and heterozgous carriers of a *Fah* mutation (64 ng/ml avg.).

Figure 2-5. Bar graph showing SA levels in urine of *fah*^{5961SB}, *fah*^{6287SB} and control mice. *1, results were pooled for mutants ages 2 days (N=1), 7 days (N=1), 9 days (N=3), and 11 days (N=4); *2, results for mutants ages 0 (N=6); *3, results pooled for controls ages 2 days (N=1), 7 days (N=1), 9 days (N=1), 11 days (N=5) for comparison with *fah*^{6287SB} mutants, results pooled for controls ages 0 (N=2) for comparison with *fah*^{5961SB} mutants. At day 0, *fah*^{5961SB} mutant mice had a mean SA concentration of 552ng/ml, whereas wild-type mice averaged 36ng/ml. The *fah*^{6287SB} mice (ages 2-11) had a mean SA concentration (1851 ng/ul avg.) significantly greater than the mean SA concentration (68 ng/ul avg.) of control mice in the same age range. The *y-axis* represents SA concentration in ng per ml of urine, N denotes sample size, and standard error bars are shown.


2500
2000
1500
1000
500
0
SA (ng/ml urine)
N=9
N=8
N=6
N=2
fah6287SB *1
fah5961SB *2
Control *3

DISCUSSION

Hereditary tyrosinemia type 1 is a severe liver disease caused by a deficiency in FAH; despite the clinical form, patients usually succumb to generalized liver failure, disease related complications and death[1,6]. The ENU-generated mutations *5961SB* and *6287SB* cause the *Fah* deficiency that leads to neonatal death in mice. The acute form of human HT1 is characterized by severe symptoms due to the lack of FAH enzymatic activity, and is modeled by the phenotype of *fah*^{5961SB}, whereas chronic patients have milder features and reduced FAH levels[6] as seen in *fah*^{6287SB} mice.

The *fah*^{5961SB} mouse has a mutation in a consensus sequence required for correct pre-mRNA splicing, resulting in aberrant splicing with the loss of exon 7, an altered translational reading frame, and the introduction of a premature termination codon. An altered reading frame and a premature stop codon usually result in the production of truncated protein and a reduction in mRNA abundance[37,38]; misspliced RNAs are often unstable, and RNAs that harbor premature stop codons are usually degraded by cell defense mechanisms developed to preclude the formation of deleterious proteins[38]. The *fah*^{5961SB} mutation was analyzed for its effect on the level and processing of the *Fah* mRNA, and only minute amounts of normal-sized *Fah* mRNA could be detected by northern blotting. The low template *Fah* mRNA levels should have a direct effect on Fah protein abundance, and if the remaining alternatively spliced transcripts from the *fah*^{5961SB} mutation were translated, it would likely result in a structurally and/or functionally abnormal protein. The *fah*^{5961SB} mouse dies shortly after birth due to the lack of Fah enzymatic activity, making *fah*^{5961SB} a model for the acute form of HT1. In fact,

the altered transcript produced by *fah*^{5961SB} is identical to a transcript produced by a FAH mutant allele causing HT1[16].

In the *fah*^{6287SB} mouse mutant a missense mutation (A→G) in exon 6 was identified that changes a glutamic acid to a glycine at codon 201 (E201G). Glutamic acid^{201} is conserved in human, rat and mouse Fah, which may reflect an essential requirement for this amino acid at that position. Glutamic acid has a very polar acidic side chain; glutamic acids are nearly always found on the outside of protein molecules, whereas glycine has a nonpolar side chain common to the inside of proteins. This substitution could adversely affect protein stability and/or enzyme activity of the Fah protein. There are no structural data on Fah, and the role of residue 201 has not been investigated; however, this amino acid presumably plays a role in the normal function of the enzyme. This E201G mutation is located only six amino acids downstream from the location of a missense mutation known to cause HT1 (G207D)[17], which may suggest that the region represents a critical domain in the polypeptide. The *fah*^{6287SB} mutation was analyzed for its effect on the level of Fah mRNA, and was found to cause a slight reduction in mRNA levels. The mutation could be located in sequences essential for the efficient transcription of the gene or the altered transcript may have a half-life different from its normal counterpart. The lower amount of Fah mRNA may correlate with the reduced Fah activity, and also the stability and/or the translational efficiency of the mRNA may be involved. The *fah*^{6287SB} mutants live into the third week of life, suggesting the presence of low levels of Fah activity, making *fah*^{6287SB} a murine model for the chronic form of HT1.

In humans, the primary deficiency of FAH leads to the accumulation of the alkylating metabolites MAA and FAA, which are believed to be responsible for the liver and kidney damage found in HT1[1,6]. Reduction and decarboxylation of these metabolites *in vivo* results in the production of SA. SA accumulation is the indirect result of the complete or incomplete block of the FAH enzyme, and its accumulation has been linked to certain pathological aspects of the disorder[1,2,39,40]. Elevation of SA above normal levels (in serum, urine, and/or amniotic fluid) is indicative and specific for the HT1[6,7,41], so that measurement of SA is used as a diagnostic tool for HT1[9,41,42].

We report increased levels of SA in the urine of *fah*^{5961SB} and *fah*^{6287SB} mice, confirming that the mutations are affecting Fah activity, thus causing an accumulation of the toxic metabolites, FAA and MAA. GC/MS was used to provide identification and quantification of SA in the complex profiles of urinary organic acids[36,42]. Urine collected shortly after birth from *fah*^{5961SB} mice had, on average, 15X higher SA levels (552 ng/ml) then same age controls (36 ng/ml). Urine collected from various age *fah*^{6287SB} mice had on average 27X higher SA levels (1850 ng/ml) than control mice (68 ng/ml). Variation in SA levels existed between animals, which is consistent with the finding that SA levels in HT1 patients can vary considerably[36,42]. Our SA data also suggest that the neonatal lethality in the mice is not directly correlated with the amount of toxic metabolite accumulation (which is related to SA levels). SA levels in *fah*^{5961SB} mice are, on average, considerably lower just hours before death than the levels found in *fah*^{6287SB} mice that live much longer. Since *fah*^{5961SB} mice die within hours of birth, they may not have sufficient time to accumulate the higher levels of SA (a two-day-old *fah*^{6287SB} mutant had an SA

level comparable to the neonatal *fah*^{5961SB} mice). The data suggest that the *fah*^{6287SB} mutants accumulate higher levels of urinary SA due to their longer lifespan. Heterozygotes for either mutation do not exhibit an increase in SA levels, confirming that SA accompanies the disease state[42].

In conclusion, we are proposing that the ENU-generated mutants *fah*^{5961SB} and *fah*^{6287SB} are improved mouse models for the acute and chronic forms of HT1, respectively, and that all phenotypic effects are attributable to Fah deficiency alone. The *fah*^{5961SB} and *fah*^{6287SB} mice represent ideal systems to assess the therapeutic effects of drugs and diets on disease progression and expression, and the evaluation of gene therapy approaches.

MATERIALS AND METHODS

Mice. The generation at Oak Ridge National Laboratory, Biology Division of the ENU-induced mutant alleles studied has been described[23,33]. Briefly, BALB/cRl (albino, *c* / *c*) males treated with ENU were mated to (C57Bl/10Rl x C3Hf/Rl) G_0 females (+ / +). Females carrying the mutagenized paternal chromosome 7 were then mated to males that carry a long *c*-region deletion (c^{ch} / c^{26DVT}; c^{ch} is the *chinchilla* allele at *c*, and c^{ch}/*c* gives a light chinchilla coat color). Albino G_2 progeny were examined for mutations (m) because this phenotypic class carries the mutagenized chromosome 7 opposite the deficiency chromosome (*c* m / c^{26DVT}). Both *fah*^{5961SB} and *fah*^{6287SB} are evident in hemizygous (*c* m / c^{26DVT}) and homozygous states (*c* m / *c* m). The mutations are maintained by crossing heterozygous carriers (*c* m / c^{ch} +) since the hemizygous and homozygous states result in neonatal lethality. Newborn mutants lack eye pigment and can be distinguished from pigmented heterozygous carriers of the mutation and wild-type littermates.

RNA Isolation and Northern Blot Analysis. Total cellular RNAs were isolated from livers of BALB/cRl albino mice (*c* / *c*), hemizygous *fah*^{5961SB} mutants (*c fah*^{5961SB} / c^{26DVT}), *fah*^{5961SB} carrier mice (*c fah*^{5961SB} / c^{ch} +), homozygous *fah*^{5961SB} mutants (*c fah*^{5961SB} / *c fah*^{5961SB}), and wild-type littermates (c^{ch} + / c^{ch} +). The corresponding *fah*^{6287SB} RNAs were also isolated. RNAs were isolated using the TRIzol procedure (GibcoBRL), according to the manufacturer's instructions, and were analyzed by standard procedures[44,45]. Ten μg RNA were loaded into each lane, electrophoresed through a

formaldehyde-containing gel (1.0% agarose), transferred onto a nylon membrane (Duralon-UV membrane, Stratagene), and hybridized with a full-length murine *Fah* cDNA[19], labeled with [γ-^{32}P]ATP using the random primer method. Hybridization was carried out at 42°C overnight in 10X SSCP, 2% SDS, 10% dextran sulfate, and 50% formamide. Washing stringency was .5X SSCP,.1% SDS at 65°C. Loading was determined by reprobing each of the blots with a β-actin cDNA.

cDNA Production, PCR and Sequencing. Double stranded cDNAs (~1.4kb) were produced by reverse transcription of total murine liver RNA followed by PCR amplification using gene-specific oligonucleotides (5'-GCCCGGTGCTCGTCAGC ATGTCC-3' and 5'-AGCATGATCCTCATAAGGCAAGGG-3'). The amplification was performed over 35 cycles, each cycle consisting of 30 sec denaturation at 94°C, 2 min annealing at 60°C and 4 min extension at 72°C. PCR-amplified products were cloned into the plasmid vector pCRII provided in a One-Shot TA Cloning Kit (Invitrogen) and sequenced. Sequencing of control (*c* / *c*) and mutant (*c* m / c^{26DVT}) cDNAs was performed manually on both cDNA strands by the dideoxy chain-termination method[46] using synthetic oligodeoxynucleotides as primers and a Sequenase Version 2.0 DNA Sequencing kit (United States Biochemical).

PCR Amplification of Genomic DNA and Sequencing. Genomic DNA was isolated from the livers of a fah^{5961SB} hemizygous mutant and a BALB/cRl control mouse. A 100ng portion of mutant and control genomic DNA was amplified by PCR over 35

cycles, each cycle consisting of 30 sec denaturation at 94°C, 2 min annealing at 60°C and 3 min extension at 72°C. Oligonucleotides flanking the 6th intervening sequence (IVS6, 5'-GTGTATGGTGCCTGCAGACT-3' and 5'-TTCATGAGGACCATCCCG-3') were used as primers in the PCR assay to amplify a ~1.6 kb DNA fragment that included IVS6. Amplified DNA was purified by low-gelling temperature gel electrophoresis, and the desired fragments excised from the gel and further purified using the Wizard PCR Prep DNA purification system (Promega). The purified DNA fragments were cloned into the plasmid vector pCRII provided in a One-Shot TA Cloning Kit (Invitrogen) and sequenced (primers 5'-CATGTGAGTAGAGTTCCCAC-3' and 5'-GGGCTTTGGAAATGGGGA-3') using the ABI PRISM Dye Terminator Cycle Sequencing Kit (ABI373, Perkin Elmer), according to the manufacturer's instructions.

Biochemical Analysis. Urine from *fah*^{5961SB} and *fah*^{6287SB} mutants, heterozygous carriers, and wild-type siblings was collected and stored at -20°C.

Extraction and Derivatization of SA: The SA was first oximated using a modification of the procedure of Tuchman[47]. HPLC-grade water (0.3 ml), hydroxylamine hydrochloride (0.2 ml, 200 mg/ml in water), HCl (40 µl, 6 M), and mouse urine (5 to 100 µl) were added to 4 ml ReactiVials. The samples were spiked with 5µl of oximated 5,7-dioxooctanic acid (Ox-DOOA: 40 µg/ml in methanol) as an internal reference. (DOOA is a homolog of SA and contains an additional CH_2 group). The samples were heated at 80°C for 30 min to oximate the SA present and convert it to 5(3)-methyl-3(5)-isoxazole propionic acid. After cooling, the samples were extracted twice with 3 ml ether each

time. (In earlier extractions, NaCl was added to saturate the samples with salt[36], but this was found to be unnecessary for good recoveries of Ox-SA.) The ether extracts were gently blown to dryness at 40°C using nitrogen. To form the tert-butyl-dimethylsilyl derivative of the Ox-SA, 20 µl of N-methyl-N-(tert-butyldimethylsilyl)trifluoracetamide (MTBSTFA) and 20 µl of pyridine was added to each vial. The samples were vortexed in 2 ml ReactiVials and heated at 80°C for 30 min.

Gas Chromatography / Mass Spectrometry: Analyses were carried out using a Hewlett Packard 5890 Series II GC interfaced to a 5989A Mass Spectrometer. An HP 5-MS (crosslinked 5% diphenyl 95% dimethylsiloxane) capillary column (30 m x 0.25 mm x 0.25 µ film) was used for the chromatographic separations. The injector and detector were set at 250°C and 280°C respectively. The source and analyzer were set at 200°C and 100°C respectively. The initial column temperature was 140°C, held for 5 min, then ramped at 15°C/min to 260°C and held for 3 min. The injections (1 µl) were splitless, with the purge valve turned on at 1 min. The oximated and derivatized analytes were detected by selected ion monitoring (SIM) using 212 and 138 m/z ions for SA and 226 and 152 m/z ions for DOOA.

REFERENCES

1. Goldsmith, L.A., Laberge, C. Tyrosinemia and related disorders. *The metabolic basis of inherited disease* (McGraw-Hill, New York, 6th ed. Vol. 1, 547-562, 1989).

2. Berger, R., van Faassen, H., Smith, G.P.A. Biochemical studies on the enzymatic deficiencies in hereditary tyrosinemia. *Clinica Chimica Acta* **134**, 129-141 (1983).

3. Overturf, K. *et al.* Hepatocytes corrected by gene therapy are selected *in vivo* in a murine model of hereditary tyrosinemia type 1. *Nature Genet.* **12**, 266-273 (1996).

4. Tanguay, R.M. *et al.* Different molecular basis for fumarylacetoacetate hydrolase deficiency in two clinical forms of hereditary tyrosinemia (type 1). *Am. J. Hum. Genet.* **47**, 308-316 (1990).

5. Labelle, Y., Phaneuf, D., Leclerc, B., Tanguay, R.M. Characterization of the human fumarylacetoacetate hydrolase gene and identification of a missense mutation abolishing enzymatic activity. *Hum. Mol. Genet.* **2** (7), 941-946 (1993).

6. Kvittingen, E.A. Hereditary tyrosinemia type 1 - an overview. *Scand. J. Clin. Lab. Invest.* **46** (184), 27-34 (1986).

7. Pettit, B.R., MacKenzie, F., King, G.S. The antenatal diagnosis and aid to the management of hereditary tyrosinaemia by use of a specific and sensitive GC-MS assay for succinylacetone. *J. Inher. Metab. Dis.* **7** (2), 135-136 (1984).

8. Grenier, A., Lescault, A., Laberge, C., Gagne, R., Mamer, O. Detection of succinylacetone and the use of its measurement in mass screening for hereditary tyrosinemia. *Clinica Chimica Acta* **123**, 93-99 (1982).

9. Linstedt, S., Holme, E., Lock, E.A., Hjalmarson, O., Strandvik, B. Treatment of hereditary tyrosinaemia type 1 by inhibition of 4-hydroxyphenylpyruvate dioxygenase. *Lancet* **340**, 813-817 (1992).

10. Phaneuf, D. *et al.* Cloning and expression of the cDNA encoding human fumarylacetoacetate hydrolase, the enzyme deficient in hereditary tyrosinemia: assignment of the gene to chromosome 15. *Am. J. Hum. Genet.* **4**, 525-535 (1991).

11. Phaneuf, D. *et al.* Type 1 hereditary tyrosinemia: evidence for molecular heterogeneity and identification of a causal mutation in a French Canadian patient. *J. Clin. Invest.* **90**, 1185-1192 (1992).

12. Rootwelt, H. *et al.* Two missense mutations causing tyrosinemia type 1 with presence and absence of immunoreactive fumarylacetoacetate. *Hum. Genet.* **93**, 615-619 (1994).

13. Rootwelt, H., Kristensen, T., Berger, R., Hoie, K., Kvittingen, E.A. Tyrosinemia type 1 - complex splicing defects and a missense mutation in the fumarylacetoacetase gene. *Hum. Genet.* **94**, 235-239 (1994).

14. St-Louis, M. *et al.* Identification of a stop mutation in five Finnish patients suffering from hereditary tyrosinemia type 1. *Hum. Mol. Genet.* **3** (1), 69-72 (1994).

15. St-Louis, M. *et al.* Two novel mutations involved in hereditary tyrosinemia type 1. *Hum. Mol. Genet.* **4** (2), 319-320 (1995).

16. Ploos van Amstel, J.K. *et al.* Hereditary tyrosinemia type 1: novel missense, nonsense and splice consensus mutations in the human fumarylacetoacetate hydrolase gene; variability of the genotype-phenotype relationship. *Hum. Genet.* **97**, 51-59 (1996).

17. Timmers, C., Grompe, M. Six novel mutations in the fumarylacetoacetate hydrolase gene of patients with hereditary tyrosinemia type 1. *Hum. Mut.* **7**, 367-369 (1996).

18. Gluecksohn-Waelsch, S. Genetic control of morphogenetic and biochemical differentiation: lethal albino deletions in the mouse. *Cell* **16**, 225-237 (1979).

19. Klebig, M.L., Russell, L.B., Rinchik, E.M. Murine fumarylacetoacetate hydrolase (*Fah*) gene is disrupted by a neonatally lethal albino deletion that defines the hepatocyte-specific developmental regulation 1 (*hsdr-1*) locus. *Proc. Natl. Acad. Sci.* **89**, 1363-1367 (1992).

20. Ruppert, S. *et al.* Deficiency of an enzyme of tyrosine metabolism underlies altered gene expression in newborn liver of lethal albino mice. *Genes Dev.* **6**, 1430-1443 (1992).

21. Grompe, M. *et al.* Loss of fumarylacetoacetate hydrolase is responsible for the neonatal hepatic dysfunction phenotype of lethal albino mice. *Genes Dev.* **7**, 2298-2307 (1993).

22. Russell, W.L. X-ray-induced mutations in mice. *Cold Spring Harbor Symp. Quant. Biol.* **16**, 327 (1951).

23. Rinchik, E.M., Russell, L.B. Germ-line deletion mutations in the mouse: tools for intensive functional and physical mapping of regions of the mammalian genome. *Genome Analysis* (Vol 1: Genetic and Physical Mapping. Cold Spring Harbor Laboratory Press, 1990).

24. Russell, W.L. *et al.* Specific-locus test shows ethylnitrosourea to be the most potent mutagen in the mouse. *Proc. Natl. Acad. Sci.* **76** (11), 5818-5819 (1979).

25. Russell, L.B., Montgomery, C.S., Raymer, G.D. Analysis of the albino-locus region of the mouse: IV. characterization of 34 deficiencies. *Genetics* **100**, 427-453 (1982).

26. Gluecksohn-Waelsch, S. Regulatory genes in development. *TIG* **3** (5), 123-127 (1987).

27. Grompe, M. Pharmacological correction of neonatal lethal hepatic dysfunction in a murine model of hereditary tyrosinemia type 1. *Nature Genet.* **10**, 453-460 (1995).

28. Ruppert, S. *et al.* Two genetically defined trans-acting loci coordinately regulate overlapping sets of liver-specific genes. *Cell* **61**, 895-904 (1990).

29. Niswander, L. *et al.* Molecular mapping of albino deletions associated with early embryonic lethality in the mouse. *Genomics* **9**, 162-169 (1991).

30. Kelsey, G. *et al.* Physical mapping of the albino-deletion complex in the mouse to localize *alf/hsdr-1*, a locus required for neonatal survival. *Genomics* **14**, 275-287 (1992).

31. Schedl, A. *et al.* Chromosome jumping from flanking markers defines the minimal region for alf/hsdr-1 within the albino-deletion complex. *Genomics* **14**, 288-297 (1992).

32. Kelsey, G. *et al.* Rescue of mice homozygous for lethal albino deletions: implications for an animal model for the human liver disease tyrosinemia type 1. *Genes Dev.* **7**, 2285-2297 (1993).

33. Rinchik, E.M., Carpenter, D.A., Selby, P.B. A strategy for fine-structure functional analysis of a 6- to 11-centimorgan region of mouse chromosome 7 by high-efficiency mutagenesis. *Proc. Natl. Acad. Sci.* **87**, 896-900 (1990).

34. Rinchik, E.M., Carpenter, D.A. *N*-ethyl-*N*-nitrosourea-induced prenatally lethal mutations define at least two complementation groups within the embryonic ectoderm development (*eed*) locus in mouse chromosome 7. *Mammal. Genome* **4**, 349-353 (1993).

35. Holdener, B.C. *et al.* Physical location of *eed*: a region of mouse chromosome 7 required for gastrulation. *Genomics* **27**, 447-456 (1995).

36. Schierbeek, H., Berger, R. Determination of succinylacetone and succinylacetoacetate in physiological samples as the common product 5(3)-methyl-3(5)-isoxazole propionic acid using an isotope dilution method and mass spectrometry. *Clinica Chimica Acta* **184**, 243-250 (1989).

37. Dietz, H.C. *et al.* The skipping of constitutive exons *in vivo* induced by nonsense

mutations. *Science* **259**, 680-683 (1993).

38. Maquat, L.E. Defects in RNA splicing and the consequences of shortened translational reading frames. *Am. J. Hum. Genet.* **59**, 279-286 (1996).

39. Sassa, A., Kappas, A. Hereditary tyrosinemia and the heme biosynthetic pathway. *J. Clin. Invest.* **71** (3), 625-634 (1983).

40. Mitchell, G. Neurological crises in hereditary tyrosinemia. *N. Engl. J. Med.* **322**, 432-437 (1990).

41. Tuchman, M. *et al.* Persistent succinylacetone excretion after liver transplantation in a patient with hereditary tyrosinemia type 1. *J. Inher. Metab. Dis* **8**, 21-24 (1985).

42. Grenier, A., Lescault, A., Laberge, C., Gagne, R., Mamer, O. Detection of succinylacetone and the use of its measurement in mass screening for hereditary tyrosinemia. *Clinica Chimica Acta* **123**, 93-99 (1982).

43. Divry, P., Vianey-Liaud, Cotte, J. Routine gas chromatographic/mass spectrometric analysis of urinary organic acids: results over a three-year period. *Biomed. Environ. Mass Spectrom.* **14** (11), 663-668 (1987).

44. Maniatis, T., Fritsch, E.F., Sambrook, J. eds. *Molecular Cloning: A Laboratory Manual.* (Cold Spring Harbor Lab., Cold Spring Harbor, NY. 1982).

45. Ausubel, F.M. *et al. Current Protocols in Molecular Biology* (Wiley, New York, Vol. 1, 1989).

46. Sanger, F., Nicklen, S., Coulson, A.R. *Proc. Natl. Acad. Sci.* USA **74**, 5463-5467 (1977).

47. Tuchman, M. *et al.* Determination of urinary succinylacetone by capillary gas chromatography. *J. Chromatogr. Sci.* **22**, 211-215 (1984).

Rinchik, E.M. *et al.* Mouse chromosome 7. *Mammal. Genome* **3**, S104-S120 (1992).

Appendix A

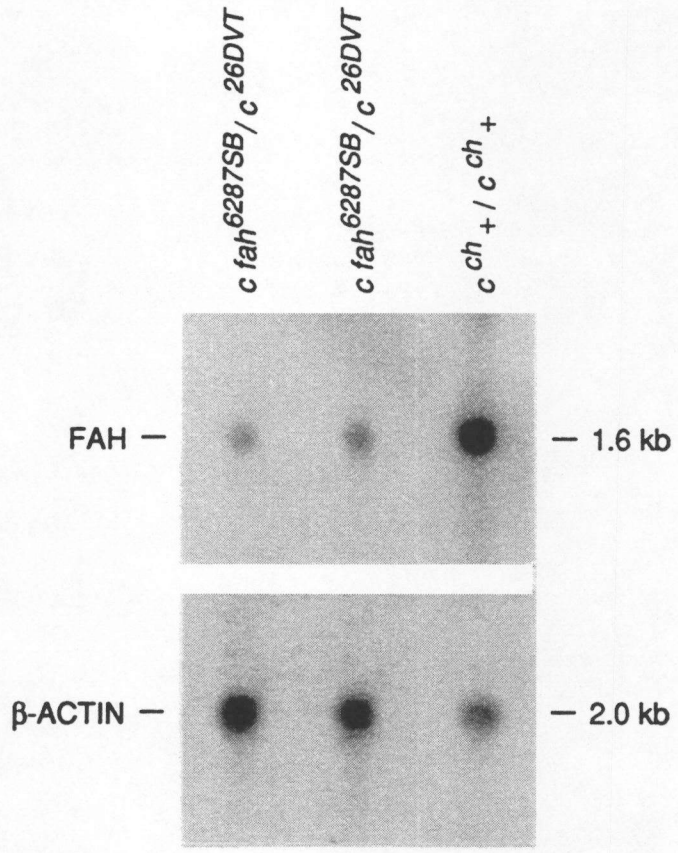
Supplemental Data

Figure A-1. Analysis of *fah*^{5961SB} and BALB/cRl cDNAs. RT-PCR amplified fragments were analyzed by electrophoresis; all lanes are labelled at the *top*. RT $^{+}$ signifies the use of reverse transcriptase in the reaction mixture, and RT $^{-}$ signifies the absence of the enzyme. The absence of fragments from the RT $^{-}$ lanes indicates a DNA free reaction. ϕX174 DNA and 1 kb DNA ladders were used to determine fragment size. The BALB/cRl cDNA is ~500 bp and the *fah*^{5961SB} cDNAs are ~400 bp's.



ΦX174 DNA Ladder
BALB/cRl control, RT^+
BALB/cRl control, RT^-
fah^{5961SB} mutant, RT^+
fah^{5961SB} mutant, RT^-
fah^{5961SB} mutant, RT^+
fah^{5961SB} mutant, RT^-
1 kb DNA Ladder

Figure A-2. Northern blot analysis of liver RNA from *fah*^{6287SB} mice. The genotype of each animal is given at the *top* and the probe used is given to the *left* of each blot. Each lane contains 10μg of total liver RNA probed with a ^{32}P-labelled *Fah* cDNA and reprobed with a β-actin probe. Size (in kb) of the major transcript identified by each probe is indicated.


c fah6287SB/c 26DVT
c fah6287SB/c 26DVT
c ch+/c ch+
FAH
1.6 kb
β-ACTIN
2.0 kb

VITA

Jennifer Lynn Aponte was born on November 9, 1970 in Long Island, New York She attended East Islip High School in East Islip, New York and graduated in June 1988. The following Fall she attended the Florida Institute of Technology, Melbourne, Florida where she received a Bachelor of Science degree in Molecular Biology and a Bachelor of Science degree in Marine Biology in May of 1993. She then obtained employment with the Pall Corporation, Glen Cove, New York in the microscopy department. In August of 1994 she began her graduate studies at the University of Tennessee-Oak Ridge Graduate School of Biomedical Sciences located in the Biology Division of Oak Ridge National Laboratory, Oak Ridge, Tennessee. She received her Masters of Science degree with a concentration in Genetics in May of 1997 for the research performed under the direction of Dr. Dabney K. Johnson. She then moved to Cary, North Carolina to pursue employment in the field of Genetics and/or Molecular Biology.